THE IDENTIFICATION OF NOVEL GENES INVOLVED IN COPPER AND OXYGEN METABOLISM

A Dissertation

presented to

the Faculty of the Graduate School

at the University of Missouri-Columbia

In Partial Fulfillment

of the Requirements for the Degree

Doctor of Philosophy

By: Nikita S. Gudekar

Dissertation Supervisor: Dr. Michael J. Petris

December. 2020

The undersigned, appointed by the Dean of the Graduate School, have examined the dissertation entitled:

THE IDENTIFICATION OF NOVEL GENES INVOLVED IN COPPER

AND OXYGEN METABOLISM

presented by **Nikita S. Gudekar**, a candidate for the degree of Doctor of Philosophy, and hereby certify that, in their opinion, it is worthy of acceptance.

Professor Dr. Charlotte Phillips

Professor Dr. David Mendoza-Cózatl

Professor Dr. Laurie Erb

Professor Dr. Gary Weisman

Professor Dr. Michael Petris

Acknowledgements

Undertaking Ph.D. studies was a life changing experience for me, and I would like to thank everyone who has guided and supported me throughout my journey.

First and foremost, I would like to express my deepest gratitude to my advisor **Prof. Dr. Michael Petris** for accepting me in his lab and for providing his mentorship throughout my graduate tenure. He has been an excellent role model and honestly, I could not have asked for a better mentor. I am extremely thankful to him for his invaluable insights and brainstorming sessions which have helped me become the researcher I am today. His way to tackle the scientific obstacles and his optimistic views has always assisted me to move on with great confidence. He is very generous and has a caring attitude towards his lab members and is extremely proud of their achievements. I would like to thank him for being very patient with me, encouraging me and believing in me. This journey would not have been possible without his valuable support. Thank you Dr. Petris!

I would also like to thank all my committee members: **Dr. Charlotte Phillips, Dr. Gary A. Weisman, Dr. David G. Mendoza-Cózatl and Dr. Laurie Erb,** for their kind assistance and insightful suggestions.

I feel very fortunate to share the 5th floor space with the Weisman lab members. My sincere gratitude goes to **Mrs. Jean Camden, Mr. Lucas Woods, Mr. Kevin Muñoz Forti and Dr. Mahmoud Khalafalla** for their valuable input in my project. Because I am surrounded by such knowledgeable and friendly

people, I always had a positive and a collaborative atmosphere around me. I would specifically like to thank **Dr. Gary Weisman**. Being part of my regular lab meetings, Dr. Weisman has been quite involved in my research and his invaluable insights have helped me improve my work in many ways.

I am also grateful to former labmates, **Dr. Aslam Khan and Dr. Kimberly Jasmer,** for their helpful recommendations on my project. I really had a great time with them sharing both my *"Aha"* as well as my *"Oh no"* moments.

I would like to extend my thanks to my friends in Columbia. Thanks to **the Zambre family, the Goswami family, the Behura family, Ms. Menka, Ms. Shirin and Ms. Juhi** for always motivating me throughout my Ph.D. career. I am blessed to have a small family away from home.

I owe my deepest gratitude to my husband, **Dr. Vinit Shanbhag**, who has supported and encouraged me throughout my graduate tenure. He has been an influential person in my life and his contribution is immeasurable. He has been a constant source of motivation during all these years. I would like to thank him for his wise counsel that has made my boat sail through the graduate career smoothly.

I am also very thankful to my beloved parents-in-law, **Mr. Chandrahas Shanbhag and Mrs. Kiran Shanbhag**. They have been always kind and helpful throughout the journey. I would like to extend my appreciation to my brother-in-law **Vishal Shanbhag** and my sister-in-law **Tejasvini Shanbhag** for their love

and support. Also, thanks to my cute little nephew **Shiven Shanbhag** who makes me happy every time I see him over video calls.

Last but not least, I would like to express my heartfelt thanks to my parents, **Mr. Santosh Gudekar and Mrs. Sugandha Gudekar.** I dedicate this thesis to them for their unconditional and endless love and support. I am forever indebted to them for giving me the experiences that have made me who I am. They have been the constant source of my strength and inspiration throughout my life. This journey was impossible without you guys; I love you Aai, Baba!

I would like to extend my deepest gratitude and appreciation to my sister **Sayali Gudekar** for her unconditional affection and encouragement. She truly has been my inspiration and I am grateful to her for always being there for me as a friend. I love her and thank her with all my heart!

Table of Contents

Acknowledgments	ii
List of Abbreviations	vii
List of Figures	x
Abstract	xii
Chapter I. Introduction	1
1.1 Copper homeostasis	1
1.2 Copper acquisition in mammals	3
1.3 Intracellular copper buffering and trafficking	7
1.4 Copper trafficking to mitochondrial cytochrome c oxidase	9
1.5 Metalation of cuproenzymes within the secretory pathway	10
1.5.1 Regulation of copper export	12
1.6 Disorders of copper metabolism	14
1.7 Questions addressed in this thesis	17
Chapter II. Metallothioneins regulate ATP7A trafficking and control cell viability during copper deficiency and excess	19
Abstract	20
2.1 Introduction	21
2.2 Results	24
2.2.1 Generation of cell lines lacking *Atp7a*, *MtI* and *MtII* genes	24
2.2.2 Characterization of the ATP7A-/MT- cells	25
2.2.3 Suppressor mutations in ATP7A-/MT- cells increase ATP7B expression and confer copper tolerance	28
2.2.4 Metallothioneins negatively regulate Cu-stimulated trafficking of ATP7A from the Golgi	29
2.2.5 ATP7A and MTs are determinants of cell viability during copper starvation	30
2.3 Discussion	31
2.4 Experimental procedures	35
Chapter III. VHL-mediated regulation of ATP7B connects oxygen and copper metabolism	66
Abstract	67
3.1 Introduction	68
3.2 Results	70

3.2.1 Genome-wide CRISPR based screen for Cu tolerance in Cu^S cells	70
3.2.2 Disruption of the VHL gene in Cu^S cells confers Cu tolerance by stimulating expression of the ATP7B protein	72
3.2.3 Pharmacological inhibition of prolyl hydroxylases stimulates expression of the ATP7B protein	73
3.2.4 Hypoxia stimulates expression of the ATP7B protein in mice	74
3.3 Discussion	75
3.4 Experimental procedures	79
Chapter IV. Summary and future directions	94
4.1 Summary	94
4.2 Future work	98
References	102
VITA	119

List of Abbreviations

ATOX1	Antioxidant protein 1
Atp7a$^{fl/Y}$	*Atp7a* floxed
BCS	Bathocuproinedisulfonic acid
CCS	Copper chaperone for Superoxide Dismutase
COX	Cytochrome C Oxidase
CP	Ceruloplasmin
CRISPR	Clustered regularly interspaced short palindromic repeats
CTR1	Copper transporter 1
CTR2	Copper transporter 2
Cu	Copper
Cu^{S}	Copper sensitive cell line
DAPI	4′,6-diamidino-2-phenylindole
DMEM	Dulbecco's Modified Eagle's Medium
DMT1	Divalent metal transporter
EPO	Erythropoietin

Fe	Iron
FPN	Ferroportin
gRNA	Guide RNA
GSH	Glutathione
HIF	Hypoxia inducible factor
HRE	Hypoxia response elements
ICP-MS	Inductively coupled plasma mass spectrometry
IMS	Intermembrane space
LCopA	*Legionella pneumophila*
LOX	Lysyl oxidase
MBD	Metal binding domain
MT	Metallothionein
PFA	Paraformaldehyde
PHD	Prolyl hydroxylases
ROS	Reactive oxygen species
SOD1	Superoxide Dismutase 1

Sp1	Specificity protein 1
SV40	Simian virus 40
TGN	*Trans*-Golgi network
TM	Transmembrane
VHL	von Hippel Lindau
Zn	Zinc

List of Figures

Figure	Title	Page
I-1	Model of cellular copper homeostasis in mammals	3
I-2	Schematic model of ATP7A/B structure and predicted Cu entry site	12
II-1	Derivation and characterization of cell lines lacking *Atp7a*, *MtI* and *MtII* genes	40
II-2	Disruption of *Atp7a* and *MtI/II* results in a loss of cell viability that is suppressed by Cu chelation	42
II-3	Relative contributions of ATP7A and metallothioneins to Cu tolerance	44
II-4	Selection for Cu tolerance in the absence of ATP7A increases ATP7B expression	46
II-5	Metallothionein regulates Cu-stimulated ATP7A trafficking and function	48
II-6	ATP7A and MTs decrease cell viability during Cu starvation	50
II-S1	Breeding strategy used to generate *Atp7a* floxed mice carrying deletions in *Mtl* and *Mtll* genes	52
II-S2	Deletion of the *Atp7a* gene in MT- cells causes a loss of cell viability that is rescued by Cu chelation	54
II-S3	Iron (Fe) and Zinc (Zn) concentrations in each cell line were determined by ICP-MS	56
II-S4	Deletion of *ATP7A* and *MTI/II* causes hypersensitivity to sub-micromolar Cu concentrations	58
II-S5	Deletion of *ATP7A* and *MTI/II* increases cellular GSH levels and reduces the ratio of reduced glutathione (GSH) to oxidized glutathione (GSSG)	60

II-S6	Quantitative real time PCR analysis of *Atp7a* and *Atp7b* mRNA expression in spontaneously Cu resistant cell lines	62
II-S7	Full length gels and immunoblot from Figure 1	64
II-S8	Full length gels and immunoblot from Figure 4	65
III-1	A genome-wide knockout screen identifies the von Hippel Lindau (*Vhl*) gene as a novel regulator of Cu tolerance	83
III-2	CRISPR-targeted disruption of the *Vhl* gene induces ATP7B expression at the mRNA and protein level	85
III-3	Roxadustat induces ATP7B expression in vitro and in vivo	87
III-4	Hypoxia induces ATP7B expression in vivo	90
III-S1	List of gRNAs targeting *Ctr1* and *Vhl* in Cu^S cells	92
IV-1	Proposed model for the function of ATP7B in hypoxia-induced erythropoiesis	97

THE IDENTIFICATION OF NOVEL GENES INVOLVED IN COPPER AND OXYGEN METABOLISM

Nikita Gudekar

Dr. Michael Petris, Dissertation Supervisor

Abstract

Copper (Cu) is an essential trace dietary metal which is also potentially toxic. Cells have evolved an intricate system of transporters and chaperones to carefully regulate Cu homeostasis. Cu uptake is mediated by the Cu^{1+}-specific permease, CTR1. Cytoplasmic Cu is delivered to specific compartments via a series of metallochaperones. In the *trans*-Golgi network (TGN), the ATP7A or ATP7B proteins are required to pump Cu into the secretory pathway to various cuproenzymes. ATP7A also plays a protective role against Cu toxicity by trafficking to the plasma membrane to export Cu from the cell. Metallothioneins (MTs) are another type of protein that plays a protective role against Cu toxicity by sequestering excess Cu in the cytoplasm. There are four isoforms of MT in mice of which MT I and MT II are ubiquitously expressed.

Our preliminary data demonstrates the essentiality of ATP7A, MTI and MTII in copper tolerance. We generated a fibroblast cell line in which *Atp7a*, *Mt-I*, and *Mt-II* genes were deleted (Atp7a-/Mt-), which resulted in sensitivity of these cells to sub-micromolar levels of copper. Using a genome-wide CRISPR-Cas9 deletion screen, we identified a novel

gene, *VHL* (von Hippel-Lindau), that when deleted confers Cu tolerance to Atp7a-/Mt- cells. The VHL protein is a ubiquitin-ligase responsible for the degradation of HIF transcription factors, which are the major regulators of gene expression in response to hypoxia. We show that VHL deletion confers Cu tolerance by stimulating the expression of the ATP7B copper transporter. Pharmacological inhibition of VHL-HIF1α by Roxadustat (a prolyl hydroxylase inhibitor), which is clinically used to treat anemia, conferred resistance to copper by upregulating ATP7B. Importantly, Roxadustat was found to increase hepatic ATP7B expression *in vivo*. These novel data identify a previously unknown link between copper homeostasis and oxygen sensing and have potential translational implications for the treatment of Wilson disease, a copper overload condition cause by insufficient expression of ATP7B.

Chapter I

Introduction

Reprinted from: Copper metabolism as a unique vulnerability in cancer, Volume 1868, Issue 2, Vinit C. Shanbhag, Nikita Gudekar, Kimberly Jasmer, Christos Papageorgiou, Kamal Singh and Michael J. Petris
BBA – Molecular Cell Research 1868 (2021) 118893

1.1 Copper homeostasis

Copper (Cu) is an indispensable micronutrient for the development and replication of all eukaryotes (2). Because copper cannot be created or destroyed by metabolic processes, it must be acquired from external sources. The incorporation of copper into living systems is thought to have coincided with the release of molecular oxygen into earth's early atmosphere (3, 4). By harnessing the ability of copper to cycle between two oxidation states, Cu(I) and Cu(II), cuproenzymes participate in a wide spectrum of metabolic processes, including aerobic respiration, pigmentation, iron transport, superoxide dismutation and biosynthesis of the extracellular matrix. Not surprisingly, sufficient quantities of copper are necessary to sustain the growth and development of fungi, plants and animals, however, copper is also potentially toxic when present at elevated concentrations. Under these conditions, the formation of free ionic Cu(I) within the cell can inhibit the function of enzymes by oxidizing cysteines within iron-

sulfur cluster proteins or reacting with hydrogen peroxide to produce highly-reactive hydroxyl radicals (5). Accordingly, organisms have evolved a sophisticated cadre of transporters and copper-binding proteins to control the uptake, intracellular movement, storage and efflux of copper, while simultaneously preventing formation of the free ion within the cytoplasm (Figure I-1). In mammals, copper is acquired from the diet and is absorbed across the intestinal epithelium for delivery to the liver via portal circulation. The liver is the main repository of copper in the body and serves to distribute copper to peripheral organs via the bloodstream or to excrete copper from the body via the bile (6). Once growth and development are completed, whole-body copper homeostasis is maintained by balancing the amounts of copper absorbed and excreted (7). However, pregnancy and neonatal development are stages of the mammalian life cycle that require significantly higher intakes of dietary copper to meet the metabolic demands of growth and development (8).

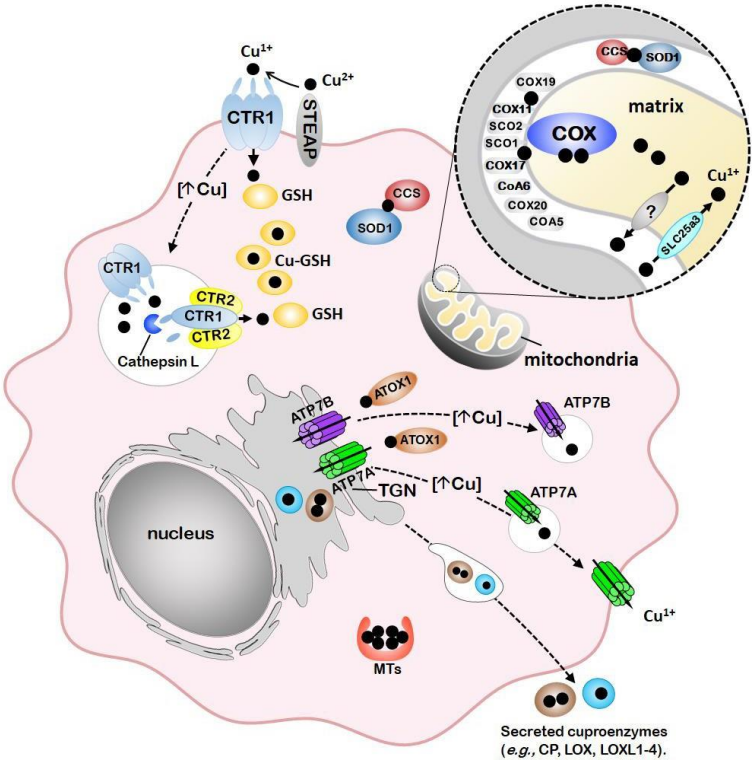

Figure I-1. Model of cellular copper homeostasis in mammals. The transport of Cu(I) (black circles) into the cytoplasm occurs via the CTR1 copper importer, which is located at the plasma membrane and within endosomal compartments. The uptake of Cu(I) via CTR1 is thought to depend on the reduction of Cu(1) to Cu(II) by members of the STEAP family of metalloreductases. The oligomerization of CTR1 and another SLC31 protein, CTR2, facilitates the cleavage of the CTR1 ectodomain by cathepsin L to enhance Cu(I) transport from endosomal compartments into the cytoplasm. Cytoplasmic Cu(I) is bound to glutathione (GSH) and can be transferred to metallochaperones for targeted trafficking to proteins. The CCS metallochaperone is required for insertion of Cu(I) into apo-SOD1 in both the cytoplasm and the mitochondrial intermembrane space. The metalation of cuproenzymes within the secretory pathway occurs via ATOX1-mediated Cu(I) delivery to the P-type ATPases, ATP7A or ATP7B, which are located in the *trans*-Golgi network (TGN) and facilitate Cu(I) loading into this organelle. Cu(I) transport into the mitochondrial matrix is facilitated by SLC25A3 located within the inner membrane. The metalation of COX occurs within the intermembrane space of the mitochondria and requires copper to be exported from the matrix via an unknown transporter. Protective mechanisms of Cu tolerance include sequestration by metallothioneins (MTs) as well as Cu(I)-stimulated trafficking of copper transporters, including the endocytosis and degradation of CTR1 which reduces Cu(I) import and exocytic trafficking of ATP7A and ATP7B to post-Golgi vesicles and the plasma membrane to facilitate copper export from the cell.

1.2 Copper acquisition in mammals

Copper uptake in mammalian cells is mediated by the CTR1 (SLC31A1) plasma membrane high affinity copper importer, which belongs to the SLC31 family of

copper permeases found in all eukaryotes (2, 9). Consistent with the essentiality of copper for normal growth and development, global deletion of the *Ctr1* gene in mice results in embryonic lethality (10). CTR1 exhibits a three-domain topology that is conserved in all members of the SLC31 family, which includes an amino terminal ectodomain containing Cu(I)-binding histidine- and methionine-rich sequences, three transmembrane domains and a cytoplasmic C-terminal tail. Biochemical studies demonstrate that SLC31 family members form functional trimers that comprise nine-membrane spanning domains that selectively permit the inward flow of Cu(I) down a concentration gradient (11, 12). Recently, the crystal structure of a CTR1 orthologue from Atlantic salmon (sCtr1) was solved, revealing a goblet-like architecture in which two rings of methionine residues were found to line the entrance to the ion conduction pore and are postulated to function as selectivity filters for Cu(I) (13). These methionine rings are created by an MXXXM motif that is conserved in the second transmembrane domain of all SLC31 family members and is essential for copper transport activity of human CTR1 (14). Another interesting feature revealed by the crystal structure of sCtr1 is the presence of an intramembranous Zn atom (13). While this could be an experimental artifact, it suggests an intriguing possibility that Zn^{2+} may be required to modulate the function of CTR1.

Approximately 95% of copper in the plasma is found within ceruloplasmin, a multicopper oxidase that facilitates cellular iron export by oxidizing Fe^{2+} as it exits the iron exporter, ferroportin (15). Although there is some evidence from cell

culture experiments that ceruloplasmin-bound copper may be used as a source of copper by CTR1 (16), the fact that aceruloplasminemic mice and humans do not exhibit copper deficiency indicates that ceruloplasmin is not a major contributor to copper uptake *in vivo* (17). Rather, minor fractions of copper bound to amino acids and other small molecular weight carriers are thought to be the major sources of plasma copper for cellular uptake (18, 19). There is evidence of an alternate copper importer, divalent metal transporter 1 (DMT1), that imports copper in some cells under conditions of high extracellular copper concentrations and this mechanism appears to be compensatory for the loss of CTR1 (20). The physiological significance of DMT1 in copper transport is not well-studied, but one study revealed that mouse intestinal knockout of DMT1 did not have any effect on intestinal copper absorption (21), as opposed to intestinal knockout of CTR1 in mice that caused severe neonatal growth defects due to the inability to absorb dietary copper (22).

Since copper uptake via CTR1 requires prior reduction to Cu(I) (11), this implicates the requirement of a metalloreductase. In the baker's yeast, *Saccharomyces cerevisiae*, the FRE1 protein is required for Cu^{2+} reduction prior to CTR1-mediated Cu^{1+} uptake (23). In mammals, the STEAP family of ferric reductases (STEAP 1 – 4) may serve this role based on the finding that forced expression of STEAP 2, 3 or 4 in cultured HEK293 cells confers cupric reductase activity and stimulates copper uptake (24) (Figure I-1). However, it remains to be

demonstrated whether the STEAP proteins facilitate copper uptake *in vivo* or whether these proteins physically interact with CTR1.

Studies in yeast, flies and worms indicate that CTR1-dependent copper uptake is regulated at the level of metal-responsive transcription (2). Transcriptional regulation of CTR1 in mammalian cells involves the zinc finger domain containing transcription factor, Specificity protein 1 (Sp1). Overexpression of Sp1 in small cell lung cancer cells resulted in increased *Ctr1* gene expression under normal copper conditions (25, 26). The zinc finger domains in the protein are required to bind to the promoter region of the *Ctr1* gene and these domains are also proposed to serve as copper sensors. Although the precise mechanism of *Ctr1* gene regulation by Sp1 is yet to be determined, it is speculated that excess copper may replace zinc ions in the zinc finger domain of the protein resulting in a conformational change compromising the binding of the protein to DNA. Mammalian orthologues of CTR1 are primarily regulated by post-translational mechanisms. Elevated copper concentrations stimulate CTR1 endocytosis and degradation as a homeostatic mechanism to reduce copper uptake (27, 28). Studies have also identified a second mechanism of CTR1 regulation that involves the proteolytic removal of its high-affinity copper-binding ectodomain (29, 30). Compared to the full-length protein, truncated CTR1 has reduced copper uptake activity at the plasma membrane, but increases copper export from endosomal compartments into the cytoplasm. The cleavage of CTR1 occurs via cathepsin proteases within endosomal compartments and requires

interactions with CTR2, which is the only other SLC31 protein in mammals. Although CTR2 was initially proposed as a low-affinity copper transporter, a recent study suggests that during the evolution of metazoans, prototypic CTR2 lost the ability to transport copper as it acquired the ability to regulate CTR1 cleavage (31). It is currently unknown whether the cleavage of CTR1 requires formation of a CTR1/CTR2 heterotrimer and whether CTR2 recruits cathepsin proteases to CTR1. Interestingly, the MXXXM-containing Cu(I) selectivity filter in CTR1 is also present in CTR2 and although mutational analyses indicate this motif in CTR2 is not required for CTR1 cleavage, it nonetheless may act as a copper sensor within endosomal compartments (30). Consistent with a role for CTR2 as a positive regulator of CTR1-mediated copper export from endosomes, deletion of CTR2 in mice causes an age-dependent hyperaccumulation of copper within various organs, with highest levels in the brain (30). Continued efforts to understand CTR2-dependent cleavage of CTR1 will be important to address how copper uptake is regulated in different tissues and under different physiological conditions or disease states.

1.3 Intracellular copper buffering and trafficking

Because copper is potentially toxic when present as the free ion, cytoplasmic concentrations of free copper are maintained at exceedingly low levels – estimated between 10^{-15} and 10^{-21} M, or less than one free copper ion per cell (32). Such an extraordinary limitation on free copper is achieved in part through

the metal-binding properties of metallothioneins and glutathione (Figure I-1). Metallothioneins are small cysteine-rich proteins that are transcriptionally induced by excess copper (and other metals) and protect against copper toxicity by irreversible sequestration within metal-thiolate clusters (33). In contrast, copper bound to reduced glutathione (GSH) can undergo facile exchange with higher affinity ligands, such as metallochaperones. Cytoplasmic concentrations of GSH are estimated to be in the millimolar range, which vastly exceed copper concentrations under steady state conditions (34). This allows GSH to function as a cytosolic copper buffer that not only prevents the formation of free copper ions, but also maintains a negative concentration gradient across the plasma membrane that drives CTR1-mediated copper uptake (35). Once in the cytoplasm, copper must be ferried to the active sites of cuproenzymes during their biosynthesis or shortly thereafter. This raises the question of how this highly reactive metal is delivered to the appropriate enzyme while avoiding adventitious interactions along the way. Nature has solved this problem with the evolution of a class of small copper-binding proteins known as metallochaperones that deliver copper to specific proteins. This process is facilitated by direct protein-protein interactions that induce metal transfer down an increasing affinity gradient (36-39).

1.4 Copper trafficking to mitochondrial cytochrome c oxidase

Mitochondria are one of the most important destinations of copper in the cell for the metalation of cytochrome c oxidase (COX), a critical enzyme that functions in aerobic respiration (Figure I-1). COX is a large multimeric complex at the terminus of the electron transport chain that transfers electrons from cytochrome c to molecular oxygen and contributes protons to the electrochemical gradient used to power ATP production. The two copper-binding subunits of cytochrome c oxidase, COX1 and COX2, are metalated during COX assembly within the intermembrane space (IMS) of the mitochondria (40), however, it is currently unknown how cytoplasmic copper enters this organelle. The source of copper for COX metalation is derived from an unknown non-proteinaceous anionic complex within the mitochondrial matrix (41). Recent studies in yeast have shown that a member of the mitochondrial carrier family, PIC2, and an iron transporter, MRS3, can transport copper from the IMS into the matrix and are necessary for COX biogenesis (42, 43). The PIC2 orthologue, SLC25A3, performs this function in mammalian cells (44), however, the mechanism by which copper is exported from the matrix into the IMS for COX biogenesis is currently unknown. The metalation and assembly of COX is a complex modular process that requires the metallochaperone COX17 and several other metallochaperones and assembly proteins (Figure I-1). Copper insertion into COX2 requires the transfer of copper from COX17 to SCO1, a membrane-spanning metallochaperone whose copper-binding site faces the IMS. This process is facilitated by several accessory proteins, including SCO2, COA6 and COX20. The insertion of copper into

COX1also requires COX17, the metallochaperone COX11 and other ancillary proteins that are yet to be identified (45).

1.5 Metalation of cuproenzymes within the secretory pathway

The majority of known eukaryote cuproenzymes are either secreted across the plasma membrane or reside within vesicular compartments, and because their active sites are lumenally oriented, copper must be inserted within the secretory pathway (46). In mammals, this process is facilitated by either ATP7A or ATP7B, copper pumps that are embedded in the *trans*-Golgi network (TGN) (Figure I-1) (47, 48). Both ATP7A and ATP7B (ATP7A/B) belong to the P1B subgroup of heavy-metal transporting P-type ATPases that harness the energy released from ATP hydrolysis to translocate metal ions from the cytoplasm across lipid bilayers. Mammalian ATP7A/B are specific for Cu(I) ions and share approximately 60% amino acid identity across their entire length, although the homology is much higher within signature motifs involved in catalysis. ATP7A/B also share a common molecular architecture that includes eight transmembrane helices, a long cytoplasmic amino terminal region containing six metal-binding MXCXXC sites, an intramembranous copper-binding CPC motif, two large cytoplasmic loops containing catalytic domains for ATP binding, phosphorylation and phosphatase activities and a cytoplasmic C-terminal region containing endocytosis signals (Figure I-2A) (49). The current model of the Cu-ATPase catalytic cycle follows the classic E1/E2 Post-Albers reaction that was originally described for the Na^+/K^+-ATPase (50), with additional information from

biochemical assays and the crystal structure of the LCopA Cu-ATPase from *Legionella pneumophila* (51). Copper transport is predicted to be initiated by the binding of Cu(I) to a conserved triad comprised of Met -Glu- Asp residues located at the entrance to the ion conduction pore (Figure I-2B), which stimulates ATP binding to the large cytosolic nucleotide binding domain. The hydrolysis of ATP and transfer of the released γ-phosphate to an aspartic acid within a conserved DKTGT motif generates a high-energy phosphorylated intermediate (E1P), which is thought to energetically favor copper translocation to intramembrane ligands, including the CPC motif (Figure I- 2A). An intrinsic phosphatase activity requiring a TGE motif within the actuator domain is coupled with the release of copper into the lumenal/extracellular space to complete the reaction cycle. One of the most notable features of LCopA is a bend in the second transmembrane domain as it emerges into the cytosol, which creates a “platform” adjacent to the Met- Glu - Asp triad at the pore opening (Figure I-2B and I-2C) (51). Positively charged residues that line the cytoplasmic face of the platform may provide a docking site for the amino terminal copper-binding domain or ATOX1 to facilitate copper transfer to the triad (Figure I-2C). Since LCopA has been solved only in the copper-free E2 conformation (51), additional configurations will be needed to decipher how copper moves from the triad to the intramembrane CPC and other sites within the transport pathway.

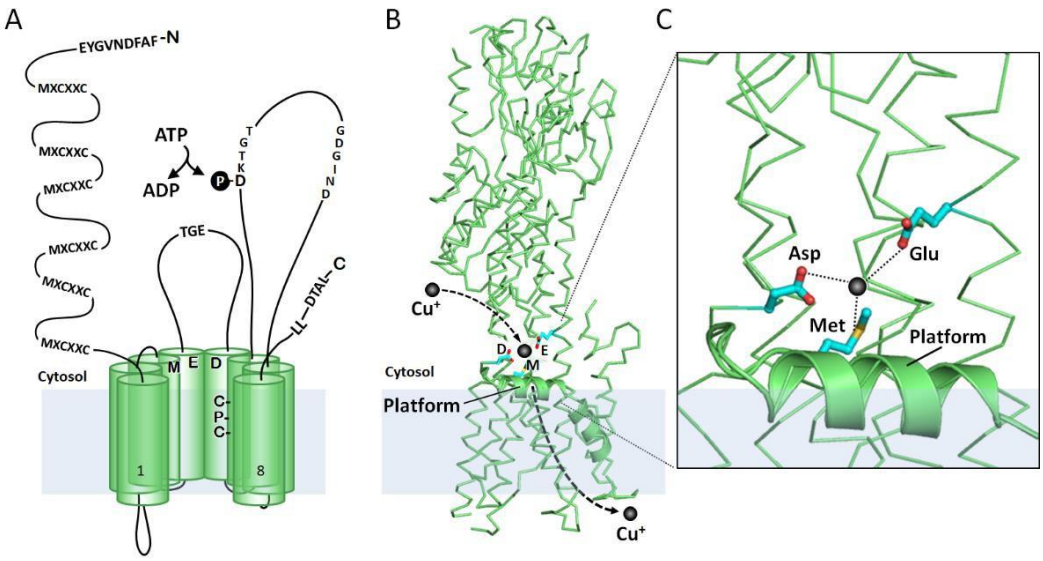

Figure I-2. Schematic model of ATP7A/B structure and predicted Cu entry site. A) Schematic illustration of ATP7A/B highlighting domains that are important for transport and trafficking function. The copper-binding MXCXXC motifs in the N-terminal domain are required for copper-induced trafficking from the TGN and to receive copper from the ATOX1 metallochaperone. Canonical sequences conserved in all P-type ATPases include the GDGIND required for ATP binding, DKTGT which contains the aspartic acid that is phosphorylated during ATP catalysis and TGE within the phosphatase domain required for removing the aspartyl phosphate. A conserved Met-Glu-Asp triad at the channel entrance and an intramembranous Cys-Pro-Cys motif are thought to coordinate copper during transport. B and C) Homology-derived structure of human ATP7A based on the crystal structure of LCopA from *Legionella pneumophila.* A bend in TM2 domain (helical ribbon) is predicted to form a platform at the cytosolic-membrane interface adjacent to the Met-Glu-Asp triad that may serve as a metallochaperone docking site for copper delivery.

1.5.1 Regulation of copper export

Cu-ATPases are found in a wide range of organisms including archaea, bacteria and eukaryotes, indicating that the requirement to transport copper was an early and constant evolutionary pressure. In addition to metalating cuproenzymes within the TGN, both ATP7A and ATP7B also export copper from cells. This process involves copper-stimulated trafficking of ATP7A and ATP7B from the TGN into post-Golgi vesicles, which are loaded with copper that is released into the extracellular milieu upon fusion with the cell surface (Figure I-1) (47, 48). Approximately 10-20% of ATP7A accumulates at the cell surface under

elevated copper conditions (52). Upon the restoration of normal copper levels, both ATP7A and ATP7B are trafficked through endosomal compartments back to the TGN via the activities of several protein complexes, including adaptor complex AP-1, retromer, Arp2/3, WASH, BLOC-1 and COMMD/CCDC22/CCDC93 complexes (53). In addition to providing a homeostatic mechanism that protects cells against rising copper levels, the exocytic trafficking of ATP7A and ATP7B in polarized cells also plays an important role in controlling systemic copper homeostasis. In intestinal epithelial cells, ATP7A traffics toward the basolateral membrane to facilitate the absorption of dietary copper (54). Whereas in polarized hepatocytes, the copper-stimulated trafficking of ATP7B controls the movement of copper into lysosomes and its subsequent release across the canalicular (apical) membrane into the bile for excretion from the body (55, 56).

Site-directed mutagenesis has identified sequences within ATP7A/B that regulate both localization within the TGN and copper-stimulated trafficking. The C-terminal domains of both ATP7A and ATP7B contain di-leucine and tri-leucine sequences (57, 58), respectively, that are required for endocytic retrieval via interactions with clathrin adaptor complexes (Figure I-2A) (59). In addition, the third transmembrane domain of ATP7A has been shown to function as an autonomous Golgi-retention signal (60). A DTAL motif at the C-terminus of ATP7A is required for basolateral targeting in polarized kidney cells (61), whereas apical targeting of ATP7B in polarized hepatoma cells requires a unique

amino acid sequence at the N-terminus (Fig 1-2A) that is absent in ATP7A (62). Copper- stimulated exocytic trafficking of ATP7A from the TGN requires at least one of the six amino terminal CXXC motifs, although one study suggests that the 5th or 6th motif closest to the membrane channel is necessary (63), whereas another study suggests any one of the six motifs will suffice (64). Mutations in different regions of ATP7A/B are known to inhibit copper-stimulated trafficking, suggesting that trafficking is coupled to the catalytic cycling. Additional studies have narrowed this requirement to the formation of the aspartyl-phosphate catalytic intermediate in both ATP7A and ATP7B (65, 66), suggesting that this conformation is recognized by sorting machinery in the TGN. Interestingly, catalysis can be uncoupled from trafficking because mutations have been identified that block copper-stimulated trafficking of ATP7A, but retain transport activity (67, 68). Future studies elucidating the phospho-intermediate structures of such mutants will aid in addressing how different catalytic conformations of ATP7A/B are recognized by sorting machinery in the TGN.

1.6 Disorders of copper metabolism

Inherited mutations that disrupt copper transport or intracellular trafficking are responsible for several human diseases. For example, certain COX deficiency disorders are caused by mutations in mitochondrial metallochaperones, such as SCO1 (OMIM 603644) (69), SCO2 (OMIM 604272) (70), COA6 (OMIM 614772) (71) and COX20 (OMIM 614698) (72). Other diseases of copper metabolism arise from mutations that impact copper absorption and its distribution in the

body. For example, loss of function mutations in *ATP7A* give rise to Menkes disease, a pediatric disorder of copper deficiency that primarily affects males due to its X-linked inheritance. Patients exhibit a wide range of defects attributable to a loss of cuproenzyme activity, including neurological degeneration, seizure, hypotonia, hypothermia, hypopigmentation and connective tissue defects (73). The deficiency of copper in affected individuals is attributable to reduced ATP7A-dependent copper export from intestinal enterocytes into the plasma, which is exacerbated by reduced copper export into the central nervous system (74, 75). Menkes patients are treated with injections of copper salts (typically copper histidinate), however, this therapy does little to improve the overall prognosis and most patients die in early childhood (76). Other treatments being actively pursued include *ATP7A* gene therapy using adeno-associated viral vectors, which have shown therapeutic efficacy in the Brindled mouse model of Menkes disease (77). The copper ionophore elesclomol is another promising treatment based on its ability to alleviate Menkes pathology and rescue mortality in the Brindled mice (78). Importantly, elesclomol has an excellent safety profile having been previously developed as an anticancer drug (79). Thus, repurposing elesclomol as a treatment for Menkes disease is an exciting prospect.

While complete loss of ATP7A function causes Menkes disease, less severe mutations in *ATP7A* give rise to occipital horn syndrome (OMIM 304150), a disease in which neurological symptoms are relatively mild and connective tissue and skeletal defects predominate (80). SMAX3 (spinal muscular atrophy X-linked

type 3; OMIM 300489) is another disorder caused by two hypomorphic missense mutations in *ATP7A*, resulting in a distal motor neuropathy, progressive gait deterioration and age-dependent muscle atrophy in the lower extremities (81). Studies in our lab have shown that motor neuron-specific deletion of *Atp7a* in mice phenocopies many of the features of SMAX3 patients, indicating that ATP7A is functionally important in this neuronal cell type (82). Two hypomorphic missense mutations in ATP7A are known to cause SMAX3 without generating a detectable copper deficiency in patients, and *in vitro* studies suggest that these mutations may impair the function of ATP7A only within motor neurons as a result of unique protein interactions in this cell type (83). It is also possible that motor neurons are more sensitive than other cell types to subtle changes in copper homeostasis caused by hypomorphic mutations in copper trafficking pathways.

In contrast to ATP7A, mutations in *ATP7B* give rise to Wilson disease in which defective ATP7B-dependent biliary copper excretion causes hepatic copper overload, which, if untreated, leads to liver failure. Wilson patients may also exhibit neurological or psychiatric symptoms due to elevated copper levels in the brain (84). Diagnostic features of Wilson disease include reduced ceruloplasmin activity and elevated copper concentrations in the serum and urine and hyperpigmented copper deposits within the cornea (Kayser-Fleischer rings) (85). The copper chelators penicillamine or trientine are often used as first-line treatments for symptomatic patients, whereas oral zinc, which is thought

to compete with dietary copper absorption, is indicated for asymptomatic patients (85). Disturbances in copper metabolism can also arise indirectly from mutations that affect general vesicular trafficking pathways. For example, in patients with MEDNIK syndrome (mental retardation, enteropathy, deafness, neuropathy, ichthyosis, keratoderma), mutations in the AP1 clathrin adapter complex give rise to hypocupremia and hypoceruloplasminemia as a consequence of defective trafficking of ATP7A and ATP7B (86). Similarly, the hypopigmentation phenotype in patients with Hermansky-Pudlak syndrome is caused by mutations affecting the BLOC-1 trafficking complex, which is required for ATP7A trafficking to melanosomes for the metalation of tyrosinase (87).

1.7 Questions addressed in this thesis

The initial aims of my Ph.D. study were to characterize the roles of ATP7A and the metallothioneins MTI and MTII in cellular copper homeostasis. In Chapter II, I describe studies in which cell lines were generated that lacked ATP7A, MTI and MTII. The absence of these proteins resulted in a synthetic lethal phenotype due to copper hyperaccumulation. In this study, we investigated the relative contribution of these copper-binding proteins during both copper deficiency and excess. Furthermore, we demonstrated a novel regulatory mechanism whereby MTs control the trafficking of ATP7A protein from the *trans*-Golgi complex in a Cu-dependent manner. Overall, this study highlights new roles for ATP7A and metallothioneins in copper homeostasis.

In Chapter III, I describe a genome-wide suppressor screen used to identify novel mutations that confer copper tolerance in cells lacking ATP7A and MTI/II. These studies reveal that mutation of the von Hippel Lindau (VHL) gene confers copper tolerance by upregulating the copper exporter ATP7B. VHL protein is a part of the E3 ubiquitin ligase complex that functions as the master regulator of oxygen sensing by controlling the abundance of the transcription factor, HIF1. Pharmacological inhibition of VHL-HIF1α by Roxadustat (a prolyl hydroxylase inhibitor), which is clinically used to treat anemia, conferred resistance to copper by upregulating ATP7B. Importantly, Roxadustat was found to increase hepatic ATP7B expression *in vivo*. These novel data identify a previously unknown link between copper homeostasis and oxygen sensing and have potential translational implications for the treatment of Wilson disease.

Chapter IV provides a summary of the major findings of this thesis and future directions.

Chapter II

Metallothioneins regulate ATP7A trafficking and control cell viability during copper deficiency and excess

As published in: Nikita Gudekar, Vinit Shanbhag, Yanfang Wang, Martina Ralle, Gary A. Weisman & Michael J. Petris; Scientific Reports volume 10, Article number: 7856 (2020)

Original link to the paper: https://www.nature.com/articles/s41598-020-64521-3

Statement of Contributions: I am the lead author on this paper. I designed and performed the majority of the experiments, including in Figures 1-6.

Abstract

Copper (Cu) is an essential, yet potentially toxic nutrient, as illustrated by inherited diseases of copper deficiency and excess. Elevated expression of the ATP7A Cu exporter is known to confer copper tolerance, however, the contribution of metal-binding metallothioneins is less clear. In this study, we investigated the relative contributions of ATP7A and the metallothioneins MT-I and MT-II to cell viability under conditions of Cu excess or deficiency. Although the loss of ATP7A increased sensitivity to low Cu concentrations, the absence of MTs did not significantly affect Cu tolerance. However, the absence of all three proteins caused a synthetic lethal phenotype due to extreme Cu sensitivity, indicating that MTs are critical for Cu tolerance only in the absence of ATP7A. A lack of MTs resulted in the trafficking of ATP7A from the *trans*-Golgi complex in a Cu-dependent manner, suggesting that MTs regulate the delivery of Cu to ATP7A. Under Cu deficiency conditions, the absence of MTs and/or ATP7A enhanced cell proliferation compared to wild type cells, suggesting that these proteins compete with essential Cu-dependent pathways when Cu is scarce. These studies reveal new roles for ATP7A and metallothioneins under both Cu deficiency and excess.

2.1 Introduction

Copper (Cu) is an essential enzymatic cofactor in organisms across all phyla (2, 88). The ability of Cu to cycle between Cu^{1+} and Cu^{2+} allows cuproenzymes to catalyze redox reactions in many different areas of metabolism (89). In eukaryotic cells, Cu is imported to the cytoplasm by members of the SLC31 family of high-affinity Cu permeases (90). This process is thought to be facilitated by Cu binding to glutathione in the cytoplasm (35). Glutathione-bound Cu is exchangeable with metallochaperones (91, 92), which are small cytoplasmic proteins that deliver Cu in a unidirectional manner to specific cuproenzymes or to Cu-transporting P-type ATPases located in the Golgi. This targeted delivery of Cu is thought to be facilitated by an increasing affinity gradient down successive Cu carriers as well as metal-dependent interactions between metallochaperones and target proteins (89, 91, 93, 94).

The same redox property that makes Cu indispensable as an enzymatic cofactor is also responsible for its toxicity when cytoplasmic concentrations become elevated. In its free ionic state, Cu can catalyze the formation of hydroxyl radicals, displace other metals from enzymes and interfere with protein folding (5, 95). Accordingly, mechanisms of Cu homeostasis have evolved to prevent free Cu ions from accumulating within the cytoplasm. Virtually all organisms are predicted to contain at least one P-type ATPase that exports Cu from the cytoplasm. In bacteria and mammalian cells, mutations that disrupt Cu-ATPases

are known to cause hypersensitivity to Cu, whereas overexpression of these transporters results in Cu resistance (95, 96). Mammals possess two Cu-transporting ATPases, ATP7A and ATP7B. ATP7A is expressed ubiquitously, whereas ATP7B is restricted to specific tissues with highest levels in hepatocytes (6). At the cellular level, both transporters are known to reside within the *trans*-Golgi network (TGN)(47, 48, 97). At this location, ATP7A and ATP7B transport Cu to nascent cuproenzymes within the secretory pathway (48, 98). Previous studies using cultured cell lines have demonstrated that elevated cytoplasmic Cu concentrations stimulate the trafficking of ATP7A and ATP7B to the plasma membrane or to endolysosomal compartments, respectively (47, 56). This trafficking response is a homeostatic mechanism that prevents the overaccumulation of potentially toxic Cu by facilitating Cu export across the plasma membrane or compartmentalization within post-Golgi vesicles/lysosomes.

Another conserved mechanism of Cu tolerance is metal sequestration by metallothioneins (MTs). These small cysteine-rich proteins have a high affinity for heavy metals, including Cu, Cd, Zn and Hg (99). In single-cell eukaryotes, MTs predominantly bind Cu and are required for tolerance to this metal (100). Mammals possess at least four distinct MT genes (MT-I through MT-IV), with MT-I and MT-II being the major isoforms that are ubiquitously expressed throughout development (101). MT-III and MT-IV are minor isoforms that are predominantly expressed in neurons and glia or in stratified epithelia, respectively (102, 103).

Both MT-I and MT-II are transcriptionally induced by heavy metals via the MTF-1 transcription factor in a Zn-dependent manner (104). MTs have been shown to bind Zn with high affinity, which can be readily exchanged for Cu (105). Cultured cells lacking MTs exhibit higher sensitivities to Cu, suggesting that MTs can protect against Cu *in vitro* (106). This concept is further supported by the finding that forced expression of MTs increases Cu tolerance in cultured cells (107). However, mice lacking both MT-I and MT-II do not exhibit an increased sensitivity to toxic levels of Cu, suggesting that MTs alone do not play a major role in Cu tolerance *in vivo* (108). The extent to which MTs are protective against Cu may be dependent on the expression of ATP7A, as the deletion of MT-I and MT-II causes embryonic lethality in mice lacking a functional ATP7A transporter (109).

In this study, we generated isogenic cell lines to examine the importance of ATP7A, MT-I and MT-II (MTs) to Cu homeostasis. Whereas the loss of MTs or ATP7A reduced cell proliferation in media containing elevated Cu concentrations, deletion of all three genes resulted in a loss of cell viability due to extreme sensitivity to endogenous Cu in the medium. Additionally, we found that the absence of MTs stimulated the trafficking of ATP7A from the *trans*-Golgi network to cytoplasmic vesicles, suggesting that MTs regulate the availability of Cu for ATP7A trafficking. In contrast to wild type cells, cells lacking MTs or ATP7A were viable under conditions of Cu scarcity, indicating that MTs and ATP7A restrict the flow of Cu to essential Cu-dependent metabolic pathways. Our

results reveal new roles for ATP7A and metallothioneins under conditions of Cu deficiency and excess.

2.2 Results

2.2.1 Generation of cell lines lacking *Atp7a*, *MtI* and *MtII* genes

To investigate the requirement for ATP7A and MTs in copper homeostasis, we used two different mouse strains to derive immortalized cell lines with deletions in the *Atp7a* gene with or without deletion of both *MtI* and *MtII* genes (Fig. II-1a). Floxed *Atp7a* male mice ($Atp7a^{fl/Y};MtI^{+/+};MtII^{+/+}$) (110) were crossed with female mice carrying deletions of both *MtI* and *MtII* genes (111) (Supplementary Fig. II-S1). A cross between heterozygous F1 males and females was then used to generate $Atp7a^{fl/Y};MtI^{-/-};MtII^{-/-}$ mice (Supplementary Fig. II-S1). Fibroblasts were isolated from the lungs of both $Atp7a^{fl/Y};MtI^{+/+};MtII^{+/+}$ and $Atp7a^{fl/Y};MtI^{-/-};MtII^{-/-}$ mice and subsequently immortalized using a plasmid encoding the SV40 large T antigen to obtain WT and MT- cell lines (Fig. II-1a). To delete the *Atp7a* gene, both cell lines were infected with an adenovirus expressing Cre recombinase (Ad-Cre) to generate ATP7A- cells ($Atp7a^{-/Y};MtI^{+/+};MtII^{+/+}$) and ATP7A-/MT- cells ($Atp7a^{-/Y};MtI^{-/-};MtII^{-/-}$) (Fig. II-1a). Surprisingly, the introduction of Ad-Cre virus into MT- cells to delete the *Atp7a* gene resulted in a complete loss of cell viability in basal medium, suggesting that the combined loss of ATP7A and both MTs results in lethality (Supplementary Fig. II-S2).

Although the endogenous Cu concentrations in basal medium are quite low (1.7 μM), we considered the possibility that the removal of ATP7A from MT- cells might cause extreme sensitivity to Cu, thus preventing their propagation in basal medium. To test this possibility, we deleted the *Atp7a* gene in MT- cells using Ad-Cre virus as before, but this time recovered the cells in basal medium containing the extracellular Cu chelator, bathocuproine disulfonate (BCS). This permitted the robust growth of ATP7A-/MT- clones, which could be propagated indefinitely in BCS-containing medium (Supplementary Fig. II-S2). PCR analysis of genomic DNA confirmed the *MtI* and *MtII* genotypes of each cell line (Fig. II-1b). The presence or absence of the ATP7A protein was confirmed by immunoblot analysis of each cell line, with tubulin serving as a loading control (Fig. II-1c). These findings suggest that loss of ATP7A and MTs causes a synthetic lethal genetic interaction due to extreme Cu sensitivity.

2.2.2 Characterization of the ATP7A-/MT- cells

To test whether the ability of BCS to rescue ATP7A-/MT- cells in basal medium was in fact attributable to Cu chelation, we tested whether the addition of equimolar Cu, Fe or Zn to the BCS-containing media could suppress the rescue of these cells. Of these metals, only Cu was found to prevent the rescue of ATP7A-/MT- cells by BCS (Fig. II-2a), thus confirming that the ATP7A-/MT- cells are inviable in basal medium due to Cu toxicity. Next, we measured the total Cu concentrations in each cell line grown in either basal medium or BCS-containing medium using inductively coupled plasma mass spectrometry (ICP-MS). Since

Cu toxicity in ATP7A-/MT- cells requires exposure to basal medium for at least 96 h, Cu measurements were performed on cells initially grown for two days in BCS-containing medium and then exposed to either basal medium or BCS-containing medium for a further 24 h. Compared to WT cells, the intracellular Cu concentrations were significantly elevated in both the ATP7A- and ATP7A-/MT- cells exposed to basal medium (Fig. II-2b). In contrast, there was no difference in Cu accumulation between WT and MT- cells exposed to basal medium (Fig. II-2b). As expected, BCS reduced the accumulation of Cu in all cell lines compared to basal medium, however, each mutant cell line still contained significantly more Cu than WT cells under these conditions (Fig. II-2c). Compared to WT cells, the mutant cell lines contained more Fe and Zn under basal and BCS conditions, however, these increases did not reach significance for every mutant (Supplementary Fig. II-S3).

To further characterize the contribution of ATP7A and MT to Cu tolerance, we assessed the viability of each cell line exposed to increasing Cu concentrations added to the media. Cells were cultured in either basal medium alone or containing 1 μM BCS with or without various Cu concentrations. After 6 days, cell survival was assayed. The results showed that the MT- cells were only marginally more sensitive to Cu as compared to WT cells (Figs. II-3a and II-3b). In contrast, the survival of ATP7A- cells was markedly decreased compared to both WT and MT- cells (Figs. II-3a and II-3b). The ATP7A-/MT- cells were completely inviable in as little as 0.25 μM Cu added to the BCS-

containing medium (Figs. II-3a and II-3b). Additional studies found that approximately 0.05 µM Cu added to medium containing 1 µM BCS was sufficient to reduce the viability of ATP7A-/MT- cells by 50% (Supplementary Fig. II-S4).

Previous studies suggest that the majority of cytoplasmic Cu is bound to glutathione, a highly abundant thiol-containing tripeptide that helps maintain the reducing potential of the cytosol (112, 113). Excess Cu concentrations are known to disrupt glutathione homeostasis by decreasing the ratio of reduced glutathione (GSH) to oxidized glutathione (GSSG) (114). Thus, we tested whether glutathione homeostasis might be disrupted by the loss of ATP7A and/or MT in cells grown in basal medium. Compared to WT cells, total GSH levels were significantly increased in both the ATP7A- and ATP7A-/MT- cell lines (Supplementary Fig. II-S5a). In the MT- cells there was a small but significant decrease in total GSH levels (Supplementary Fig. II-S5a). Notably, in each mutant cell line the ratio of GSH to GSSG was significantly decreased compared to WT cells (Supplementary Fig. II-S5b). These data indicate that the loss of ATP7A and/or MT significantly disrupts glutathione homeostasis.

Next, we performed complementation analyses by transfecting ATP7A-/MT- cells with expression constructs for human ATP7A, MTI or MTII, followed by selection in basal media supplemented with 1 µM Cu. Surviving cells were then expanded in basal media for further analysis. The forced expression of either MTI or MTII

was found to complement the growth of ATP7A-/MT- cells, albeit at a lower magnitude compared to force expression of ATP7A (Figs. II-3c and II-3d). Taken together, these findings suggest that ATP7A is the primary mediator of cellular Cu tolerance and that MTI and MTII provide secondary roles that become critical in the absence of ATP7A.

2.2.3 Suppressor mutations in ATP7A-/MT- cells increase ATP7B expression and confer copper tolerance

Over the course of our studies, we observed rare instances of Cu-resistant ATP7A-/MT- cells that spontaneously formed colonies in basal media. Because ATP7A-/MT- cells contain large deletions within the *Atp7a* and *Mtl/II* genes, we hypothesized that these suppressor mutations were not the result of genetic reversions, but rather induced alternative pathways of Cu handling. ATP7B is a Cu-transporting P-type ATPase that shares approximately 57% identity with ATP7A and has been shown to functionally replace ATP7A in cultured fibroblasts (115, 116). Thus, we screened the Cu-resistant ATP7A-/MT- cells for possible increases in ATP7B expression. The ATP7A-/MT- colonies were pooled and expanded in basal medium. A subset was further selected in basal media in which Cu concentrations were gradually increased to 20 µM over the course of 50 days while passaging cells every 2-3 days. Compared to the parental ATP7A-/MT- cells, the ATP7A-/MT- cells that were resistant to either basal medium or 20 µM Cu expressed higher levels of the ATP7B protein (Fig. II-4a and II-4b). Quantitative real time PCR analysis demonstrated that the abundance of

Atp7b mRNA was also increased in these Cu-resistant cell lines (Supplementary Fig. II-S6a). These results suggest that spontaneous overexpression of ATP7B is a mechanism for restoring Cu tolerance in ATP7A-/MT- cells.

In a separate experiment, we tested whether Cu selection would result in increased ATP7B expression in cells containing a functional ATP7A. Therefore, we passaged ATP7A+/MT- cells in media containing step-wise increases in Cu concentrations until resistance to 900 µM Cu was achieved. The Cu-resistant ATP7A+/MT- cells exhibited increased expression of both ATP7A protein (Fig. II-4c and II-4d) and *Atp7a* mRNA (Supplementary Fig. II-S6b) compared to the parental cells grown in basal medium. However, there was no increase in ATP7B protein in these Cu-resistant cells, and indeed for reasons that are unclear there was a small but significant decrease (Fig. II-4c and II-4e), which was also observed at the mRNA level (Supplementary Fig. II-S6c). These data suggest that elevated ATP7A expression is the major driver of Cu tolerance and that the selection for elevated ATP7B expression occurs in the absence of ATP7A.

2.2.4 Metallothioneins negatively regulate Cu-stimulated trafficking of ATP7A from the Golgi

Previous studies demonstrate that ATP7A confers Cu tolerance, which is coupled

with the Cu-stimulated trafficking of ATP7A from the Golgi to vesicular compartments or the plasma membrane (47). To explore the potential impact of MTs on this process, we used quantitative immunofluorescence microscopy to investigate the distribution of endogenous ATP7A protein in both WT and MT- cells. In WT cells grown in basal medium, the ATP7A protein was predominantly localized in a perinuclear region, which overlapped with the Golgi marker protein, GM130 (Figs. II-5a and II-5b). However, in MT- cells cultured in basal medium, there was a significantly greater fraction of the ATP7A protein located within cytoplasmic vesicles that extended outside of the perinuclear region to the cell periphery (Figs. II-5a and II-5b). The addition of BCS to the medium restored ATP7A to the perinuclear region in MT- cells, which overlapped with GM130 (Figs. II-5a and II-5b). These findings suggest that in the absence of MTs, there is more Cu available to stimulate trafficking of ATP7A from the Golgi. Consistent with these findings, the activity of the secreted Cu-dependent enzyme lysyl oxidase (LOX), which receives Cu from ATP7A (117), was found to be elevated in the basal media of MT- cells compared to WT cells (Fig. II-5c). Taken together, these results suggest that MTs lower the availability of Cu for ATP7A trafficking and transport.

2.2.5 ATP7A and MTs are determinants of cell viability during copper starvation

The finding that MTs restrict Cu delivery to ATP7A raises the question of whether MTs also control the availability of Cu for processes that are necessary for cell

viability during Cu deficiency. Thus, we investigated whether the presence of MTs or ATP7A affects cell propagation under conditions of Cu scarcity. WT, MT-, ATP7A- and ATP7A-/MT- cells were seeded at low densities in media containing 50 µM of the extracellular Cu chelator BCS. After 4 days, all cells remained viable (Fig. II-6a). Passaging of these cells for a further 4 days in the continued presence of BCS prevented the propagation of WT cells (Fig. II-6b). In contrast, MT-, ATP7A- and ATP7A-/MT- cells continued to propagate in BCS-containing media, with the most robust growth observed for both ATP7A- and ATP7A-/MT- cells (Fig. II-6b). These findings suggest that during Cu deficiency, ATP7A and to a lesser extent MTs restrict the availability of Cu for essential metabolic functions.

2.3 Discussion

Because Cu is highly toxic when present in the free ionic form, the maintenance of cellular Cu homeostasis must be strictly controlled. The purpose of the current study was to investigate the relative contributions of ATP7A, MTI and MTII to Cu homeostasis. Consistent with the role of ATP7A in Cu export, we found that ATP7A- cells accumulated higher levels of Cu compared to either WT or MT- cells and were more sensitive to this metal (Figs. II-2 and II-3). In contrast, the MT- cells were only marginally more sensitive to Cu at very high concentrations (>100 µM) (Fig. II-3). These findings indicate that ATP7A is the principal driver of Cu tolerance and suggest that the contribution of MTs is not essential in cells

with a functional ATP7A Cu transporter. Although both the ATP7A- and the ATP7A-/MT- cells were found to hyperaccumulate Cu to significantly greater levels than either WT or MT- cells when grown in basal media (Fig. II-2), only the ATP7A-/MT- cells were inviable under these conditions (Fig. II-3). From these results we conclude that MTs are necessary to protect cells against Cu overload caused by the absence of ATP7A. Compared to WT cells, concentrations of Fe and Zn were found to be elevated in cells lacking either ATP7A and/or MT, although these increases did not reach significance for all mutants (Supplementary Fig. II-S3). Since excess Cu is known to out-compete Fe and Zn for metalloenzymes (5, 104, 118, 119), it is possible that the accumulation of Fe and Zn in these mutant cells is attributable to Cu-mediated inhibition of export pathways for these metals.

The majority of cytoplasmic Cu is bound to glutathione, an antioxidant tripeptide present at millimolar concentrations within eukaryotic cells (112, 113). Previous studies have shown that ATP7A-null fibroblasts are sensitive to glutathione depletion, suggesting that glutathione can protect against Cu hyperaccumulation in the absence of ATP7A (120). Consistent with these studies, we found that the abundance and oxidation of glutathione were markedly increased in cells lacking ATP7A and/or MTs (Supplementary Fig. II-S5). However, since ATP7A-/MT- cells are inviable, this indicates that glutathione is unable to compensate for the loss of ATP7A and MTs. The inviability of ATP7A-/MT- cells is not because Cu concentrations exceed the binding capacity of glutathione, since GSH

concentrations are more abundant than Cu by several orders of magnitude. Rather, we postulate that in the absence of the high affinity Cu sinks provided by ATP7A and MTs, glutathione-bound Cu is too labile to prevent deleterious interactions of Cu with intracellular targets. This model is consistent with the prevailing concept of glutathione as a low affinity, high capacity Cu buffer that enables facile Cu exchange with high affinity targets such as metallochaperones, metallothionein and copper-dependent enzymes (91, 121).

Previous studies have shown that elevated cytoplasmic Cu concentrations stimulate ATP7A trafficking from the Golgi complex into vesicles that ultimately fuse with the plasma membrane (47). The initiation of Cu-stimulated ATP7A trafficking is dependent on its transport function as well as Cu delivery via the ATOX1 metallochaperone (65, 122). It was therefore notable that the Cu-dependent trafficking of ATP7A from the *trans*-Golgi and its transport activity (*i.e.*, LOX secretion) were both increased in MT- cells relative to WT cells in basal medium (Fig. II-5). This effect was not due to increased concentrations of total Cu in the MT- cells, which were identical to WT levels under basal growth conditions (Fig. II-2b). However, the finding that BCS restored ATP7A localization to the Golgi indicates that ATP7A trafficking in the absence of MT was caused by increased Cu availability. These findings suggest that when endogenous Cu is low, MTs limit Cu availability to ATP7A, thus ensuring that ATP7A trafficking is not inappropriately activated until Cu concentrations become elevated.

Our studies with ATP7A-/MT- cells prompted us to test whether ATP7A and MTs influence cell viability under conditions of Cu scarcity. In media containing the extracellular Cu chelator, BCS, wild type cells failed to propagate after two passages whereas the ATP7A-, MT-, and ATP7A-/MT- cells continued to propagate under these conditions (Fig. II-6). These data suggest that when extracellular Cu is limited, intracellular Cu is withheld from essential metabolic processes either by direct sequestration by MTs or by removal from the cytoplasm by ATP7A. Our results are consistent with *in vitro* studies demonstrating that apo-MT-II is able to rapidly extract copper ions from metallochaperones (91) and suggest that MTs act as irreversible sinks for Cu rather than serving as Cu storage pools that can be drawn upon in the absence of Cu import. Similarly, our findings suggest that ATP7A-dependent transport of Cu into the Golgi or post-Golgi vesicles is an irreversible process, rather than a means of storing Cu that can be released into the cytoplasm during Cu deficiency. Such a model may appear counterintuitive, since Cu tolerance mechanisms are expected to be non-functional during copper scarcity so that any available metal ion can be used for metabolic purposes. However, previous studies in *Saccharomyces cerevisiae* have shown that the vacuolar zinc importer, ZRC1, is induced by zinc deficiency to protect cells against a rapid influx of zinc when concentrations of this metal return to normal (123). Thus, ATP7A and MTs may similarly function to safeguard against Cu toxicity when levels of this metal are restored. These findings have implications for understanding copper metabolism during pathological Cu deficiency in humans. For example, excess

zinc intake due to accidental overdose is a risk factor for potentially lethal Cu deficiency (124-126). Because zinc induces the expression of MTs (104), the results of our study highlight a potential mechanism whereby excess MT limits Cu availability for essential processes.

The extreme sensitivity of ATP7A-/MT- cells to Cu raises the possibility of using these cells to identify novel Cu tolerance genes. Support for this concept was our finding that spontaneous overexpression of ATP7B restores Cu tolerance in ATP7A-/MT- cells (Fig. II-4). Virtually all eukaryotic metallochaperones and Cu transporters identified to date have been cloned by complementation of mutants in the baker's yeast, *Saccharomyces cerevisiae.* It is therefore likely that certain Cu homeostasis genes in complex multicellular organisms are yet to be identified. The ATP7A-/MT- cells described in our study may be useful for identifying such genes.

2.4 Experimental Procedures

Animals

All animal experimentation methods were carried out in accordance with the regulations set forth by the National Institutes of Health Office of Laboratory Animal Welfare and with the approval of the University of Missouri's Animal Care and Use Committee. *Atp7a* floxed ($Atp7a^{fl/Y}$) mice on the C57BL/6 background were generated in our laboratory, as previously described (110). *MtI* and *MtII*

double knockout mice (111) on the 129/SvJ background were obtained from the Jackson Laboratories (strain 002211). Standard breeding procedures were used to obtain mice with the genotypes *Atp7a*$^{fl/Y}$*; Mtl*$^{+/+}$*/MtII*$^{+/+}$ (127) and *Atp7a*$^{fl/Y}$*; Mtl*$^{-/-}$ */MtII*$^{-/-}$ (MT-).

Cell lines

Primary fibroblasts were obtained from WT and MT- mice by mincing freshly isolated lungs in Roswell Park Memorial Institute (RPMI) medium containing 4 mg/ml collagenase D and 2.5 mM $CaCl_2$, digesting for 1 h at 37^{o}C and then culturing at 37^{o}C in 5% CO_2 in RPMI media containing 10% (v/v) FBS, 2 mM glutamine and 100 U/ml penicillin-streptomycin. Primary WT and MT- fibroblasts were immortalized by transfection with the pSV3 plasmid expressing the SV40 large T antigen (128) using Lipofectamine 2000 (Invitrogen). Colonies were isolated and expanded in Dulbecco's Modified Eagle's Medium (DMEM) containing 10% (v/v) FBS, 4.5 g/L glucose, 2 mM glutamine and 100 U/ml penicillin-streptomycin (referred throughout as basal medium). To obtain ATP7A- and ATP7A-/MT- cell lines, the floxed *Atp7a* allele was disrupted in WT and MT- cell lines, respectively, using an adenoviral vector expressing GFP-tagged CRE recombinase (Ad-Cre-GFP 1700; Vector Biolabs). Individual clones were screened by immunofluorescence for the loss of ATP7A and then expanded. PCR was used to confirm the genotype of *Mtl* and *MtII* in all cell lines, as described (https://www.jax.org/strain/002211). ATP7A-/MT- cells were

propagated in basal media containing 50 µM of the Cu chelator bathocuproine disulfonate (BCS).

Plasmids

Expression plasmids for human *MTI* and *MTII* genes were purchased from Origene (RC205942 and RC202748, respectively). Human *ATP7A* plasmid pCMB344 was described previously (65). ATP7A-/MT- cells were complemented by transfection with the above plasmids using Lipofectamine 2000, followed by selection in basal media with 1 µM $CuCl_2$.

Cell viability analysis

Cells were seeded into 6-well trays (10^3 cells/well) into basal media containing either BCS or $CuCl_2$, as indicated in the figures. Cell survival was measured using a Crystal Violet assay, as described previously (129).

Immunoblotting and immunofluorescence microscopy

Immunoblot analysis (130) and immunofluorescence microscopy (131) were performed, as described. Antibodies used were anti-ATP7A (110), anti-tubulin (Sigma, T8328), anti-GM130 (BD Biosciences; 610822), horse radish peroxidase-conjugated anti-rabbit IgG (Santa Cruz; SC2357), anti-mouse IgG (ThermoFisher; 31430), and Alexa Fluor 488-conjugated anti-rabbit

(ThermoFisher; A11034) and Alexa Fluor 594-conjugated anti-mouse IgG (ThermoFisher; A11032). Rabbit polyclonal anti-ATP7B antibodies were produced commercially by Primm Biotech against a recombinant murine ATP7B protein comprising amino acids 316-491 and 1373-1460 connected by a spacer sequence of four glycines.

RNA isolation and quantitative PCR (qPCR)

RNA was purified using the RNeasy Plus kit (Qiagen, 74134) and cDNA was synthesized using the RNA to cDNA EcoDry kit (Takara), according to the manufacturer's instructions. Quantitative PCR analysis was performed using Taqman probes from Applied Biosystems for *Atp7a* (Mm00437663), *Atp7b* (Mm00599675) and *Gapdh* (Mm99999915).

Enzyme assays and metal measurements

Media harvested from cells after 48 h culture were used to measure lysyl oxidase activity using a LOX activity kit (Abcam, ab112139), according to the manufacturer's instructions. Metal measurements were performed using inductively coupled plasma mass spectroscopy (ICP-MS), as described previously (30). GSH and GSSG were measured using the Glutathione Colorimetric Detection Kit (Arbor Assays, K1006-H1), according to the manufacturer's protocol.

Statistical analyses

Statistical analyses were performed using GraphPad Prism 7.0. Values were expressed as mean ± standard error of the mean (SEM) and obtained from at least three biological replicates. Data were analyzed using the standard Student's *t*-test and were considered significant when $p \leq 0.05$. For multiple comparisons, a one-way analysis of variance with post-hoc Tukey test was used. Statistical significance representations: *$p < 0.05$, **$p < 0.01$, ***$p < 0.001$ and ****$p < 0.0001$.

Figures

Fig. II-1: Derivation and characterization of cell lines lacking *Atp7a*, *MtI* and *MtII* genes. (**a**) Primary fibroblasts were isolated from the lungs of *Atp7a*$^{fl/Y}$;*MtI*$^{+/+}$/*MtII*$^{+/+}$ and *Atp7a*$^{fl/Y}$;*MtI*$^{-/-}$/*MtII*$^{-/-}$ mice and then immortalized by transfection with a plasmid expressing the SV40 large T antigen (SV40 Tag) resulting in WT and MT- cells, respectively. An adenoviral vector encoding CRE recombinase was used to delete *Atp7a* in WT and MT- cells to obtain ATP7A- and ATP7A-/MT- cells, respectively. (**b**) PCR analysis of genomic DNA was used to confirm deletion of *MtI* and *MtII* genes in both the MT- and ATP7A-/MT- cell lines. Expected PCR product sizes: *MtI* gene (WT = 161 bp; knockout = 176 bp); *MtII* gene (WT = 282 bp; knockout = 299 bp). (**c**) Immunoblot analysis was used to confirm the loss of ATP7A protein in both ATP7A- and ATP7A-/MT- cell lines. Tubulin was detected as a loading control. Images of full-length gels and immunoblots are provided in the supplementary data.

Fig. II-1

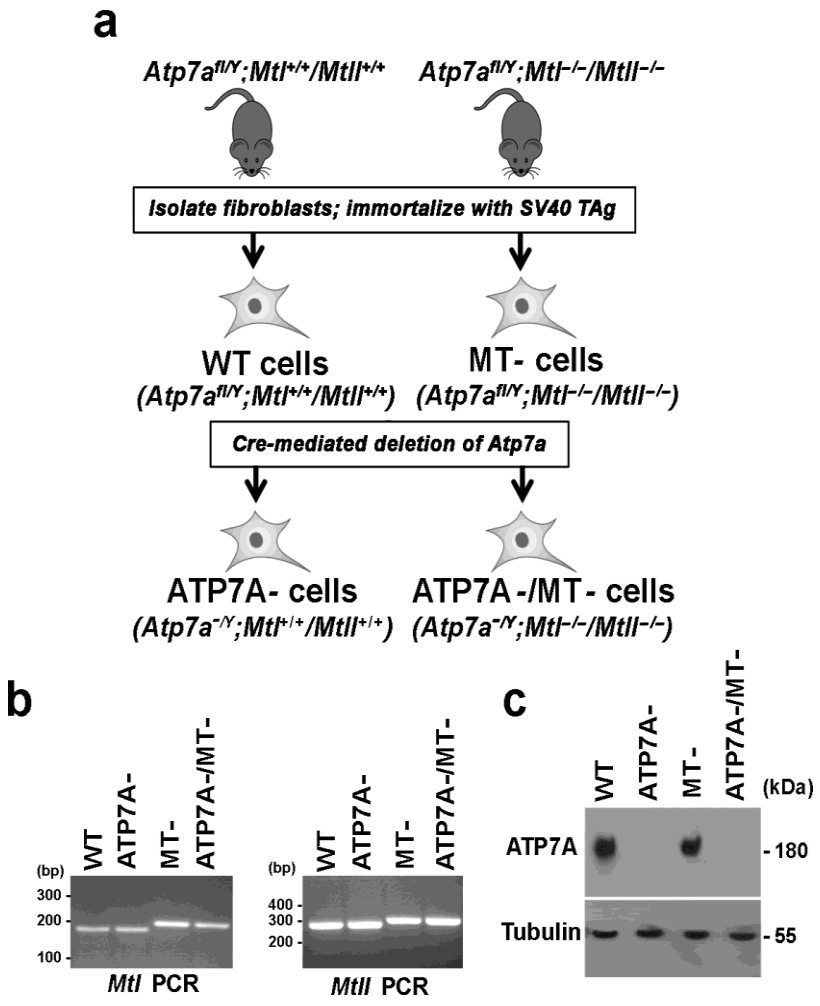
a
Atp7a^fl/Y;Mtl+/+/Mtll+/+
Atp7a^fl/Y;Mtl−/−/Mtll−/−
Isolate fibroblasts; immortalize with SV40 TAg
WT cells
(Atp7a^fl/Y;Mtl+/+/Mtll+/+)
MT- cells
(Atp7a^fl/Y;Mtl−/−/Mtll−/−)
Cre-mediated deletion of Atp7a
ATP7A- cells
(Atp7a-/Y;Mtl+/+/Mtll+/+)
ATP7A-/MT- cells
(Atp7a-/Y;Mtl−/−/Mtll−/−)
b
WT
ATP7A-
MT-
ATP7A-/MT-
(bp)
300
200
100
Mtl PCR
(bp)
400
300
200
Mtll PCR
c
WT
ATP7A-
MT-
ATP7A-/MT-
(kDa)
ATP7A
180
Tubulin
55

Fig. II-2: Disruption of *Atp7a* and *Mtl/ll* results in a loss of cell viability that is suppressed by Cu chelation. (**a**) The rescue of ATP7A-/MT- cells by the Cu chelator BCS is suppressed by copper, but not zinc or iron. ATP7A-/MT- cells were grown for 5 days in basal media containing 1 µM BCS with or without equimolar concentrations of $CuCl_2$, $ZnCl_2$ or $FeCl_2$. Cell survival was then determined using the Crystal Violet assay and imaged. (**b and c**) Cu concentrations in each cell line were determined by ICP-MS. Cells were grown for 2 days in medium containing 50 µM of the copper chelator BCS and then exposed for 24 h to either basal media or media supplemented with 50 µM BCS (mean ± SEM; *p < 0.05; **p < 0.01; ***p < 0.001; ns = not significant).

Fig. II-2

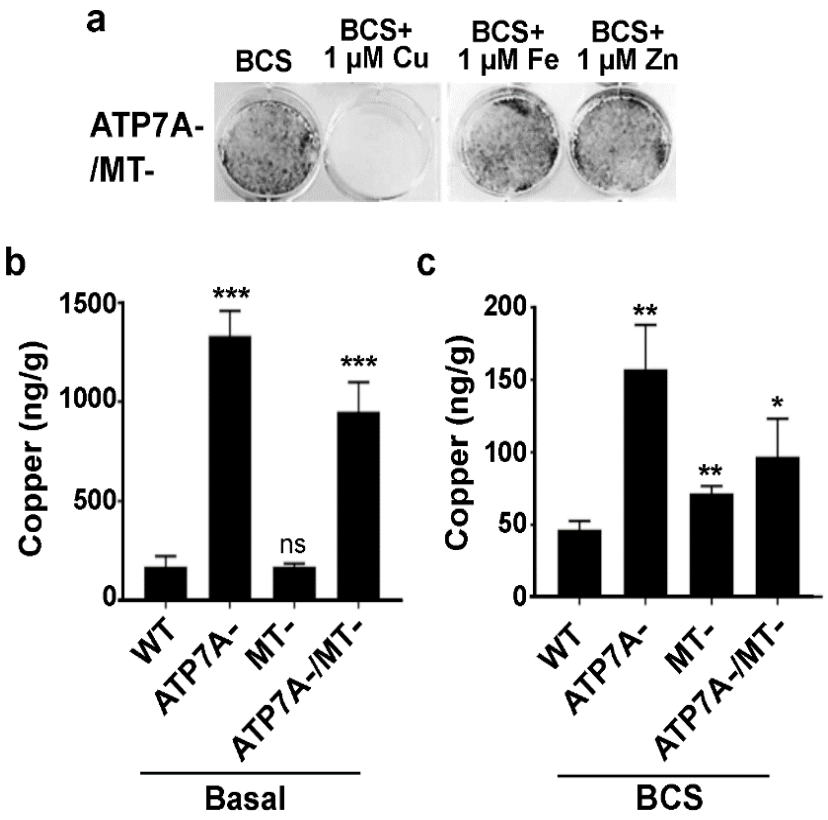
a
BCS
BCS+ 1 μM Cu
BCS+ 1 μM Fe
BCS+ 1 μM Zn
ATP7A-/MT-
b
Copper (ng/g)
1500
1000
500
0
***
ns
***
WT
ATP7A-
MT-
ATP7A-/MT-
Basal
c
Copper (ng/g)
200
150
100
50
0
**
**
*
WT
ATP7A-
MT-
ATP7A-/MT-
BCS

Fig. II-3: Relative contributions of ATP7A and metallothioneins to Cu tolerance. (**a**) Cu sensitivity of WT, ATP7A-, MT- and ATP7A-/MT- cells. For each cell line, 10^3 cells/well were seeded in 6-well plates containing basal medium, or basal medium containing 1 µM BCS with or without the indicated concentrations of $CuCl_2$. After 6 days, cell survival was determined using the Crystal Violet assay and imaged. (**b**) Quantification of Crystal Violet staining. Data are expressed as percent cell survival for each cell line normalized against its growth in BCS (mean ± SEM). (**c**) Complementation of ATP7A-/MT- cells with plasmids encoding human cDNAs for *ATP7A* (+ATP7A), *MTI* (+MTI) or *MTII* (+MTII). Cells were transfected with each plasmid and then selected in basal medium supplemented with 1 µM $CuCl_2$. Equal numbers of surviving cells (10^3 cells/well) were then seeded into 6-well plates containing basal medium, 1 µM BCS or 1 µM BCS plus the indicated concentrations of Cu. After 6 days, cell survival was determined using the Crystal Violet assay and imaged. (**d**) Quantification of Crystal Violet staining. Data are expressed as percent cell survival for each cell line normalized against its growth in BCS (mean ± SEM).

Fig. II-3

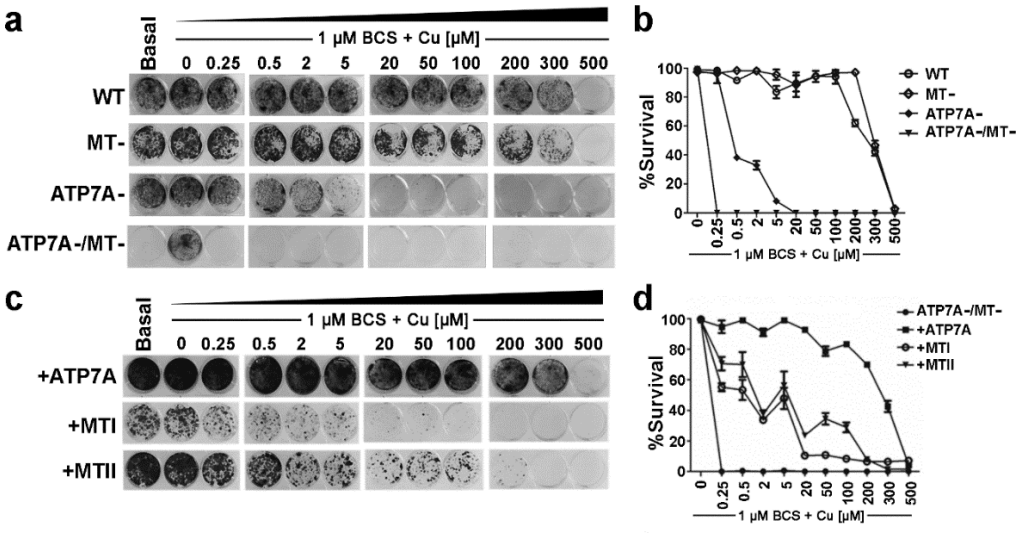
a
Basal
1 μM BCS + Cu [μM]
0 0.25 0.5 2 5 20 50 100 200 300 500
WT
MT-
ATP7A-
ATP7A-/MT-
b
%Survival
WT
MT-
ATP7A-
ATP7A-/MT-
1 μM BCS + Cu [μM]
c
Basal
1 μM BCS + Cu [μM]
0 0.25 0.5 2 5 20 50 100 200 300 500
+ATP7A
+MTI
+MTII
d
%Survival
ATP7A-/MT-
+ATP7A
+MTI
+MTII
1 μM BCS + Cu [μM]

Fig. II-4: Selection for Cu tolerance in the absence of ATP7A increases ATP7B expression. (**a**) Immunoblot detection of ATP7B in ATP7A-/MT- cells that were selected for survival in either basal media (Basal) or media containing 20 µM Cu (CuR20). The control sample is ATP7A-/MT- cells propagated in medium containing 50 µM BCS. Each cell line was grown for 16 h in basal media prior to immunoblot analysis. Tubulin was detected as a loading control. (**b**) Densitometry analysis of ATP7B protein levels normalized against control samples (mean ± SEM; *$p < 0.05$; ****$p < 0.0001$). Data were calculated from at least 3 independent experiments. (**c**) Immunoblot detection of ATP7A and ATP7B proteins in parental ATP7A+/MT- cells (Basal) or ATP7A+/MT- cells that were selected in media containing 900 µM Cu (CuR900). Both cell lines were grown for 16 h in basal media prior to immunoblot analysis. Tubulin was detected as a loading control. (**d and e**) Densitometry analysis of ATP7A and ATP7B protein levels normalized against Basal samples (mean ± SEM; *$p < 0.05$; ***$p < 0.001$). Data were calculated from at least 3 independent experiments. Images of full-length immunoblots are provided in the supplementary data.

Fig. II-4

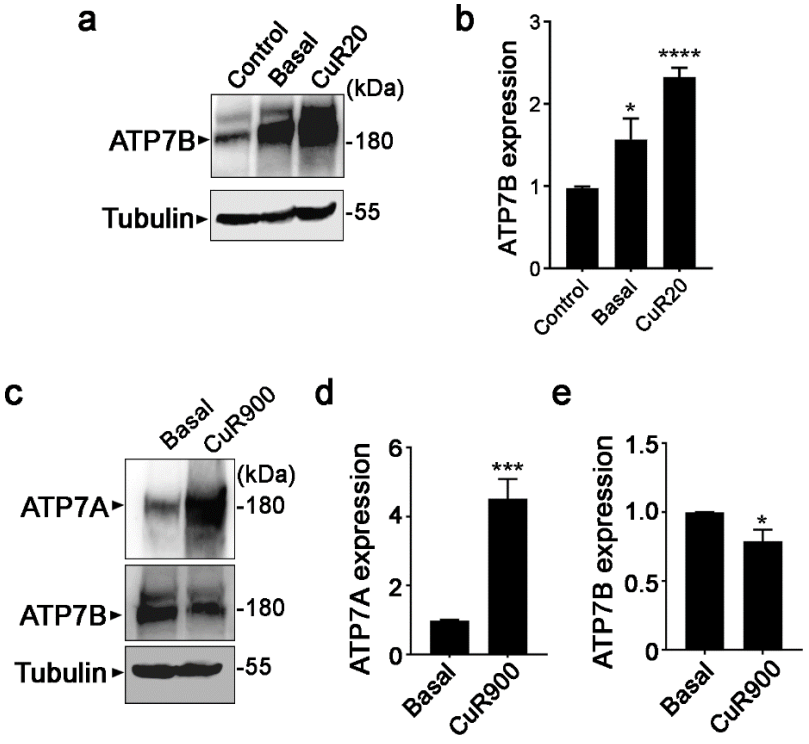
a
Control
Basal
CuR20
(kDa)
ATP7B
-180
Tubulin
-55
b
ATP7B expression
3
2
1
0
*
****
Control
Basal
CuR20
c
Basal
CuR900
(kDa)
ATP7A
-180
ATP7B
-180
Tubulin
-55
d
ATP7A expression
6
4
2
0
***
Basal
CuR900
e
ATP7B expression
1.5
1.0
0.5
0
*
Basal
CuR900

Fig. II-5: Metallothionein regulates Cu-stimulated ATP7A trafficking and function. (**a**) Immunofluorescence microscopy was performed to detect endogenous ATP7A (green) in WT and MT- cells cultured for 24 h in basal medium alone or basal medium supplemented with 50 µM BCS. Antibodies against GM130 were used to label the Golgi complex (red) and DAPI was used to stain the nuclei (blue). (**b**) The ATP7A staining intensity in the Golgi region was expressed relative to the ATP7A staining intensity within the non-Golgi region for each cell line. Values were calculated using ImageJ software (mean ± SEM; ***$p < 0.001$; ns = not significant; n = 24 cells for WT and MT- cells for each condition). (**c**) Lysyl oxidase (LOX) activity was measured in the media collected from WT and MT- cells cultured for 48 h (mean ± SEM; *$p < 0.05$).

Fig. II-5

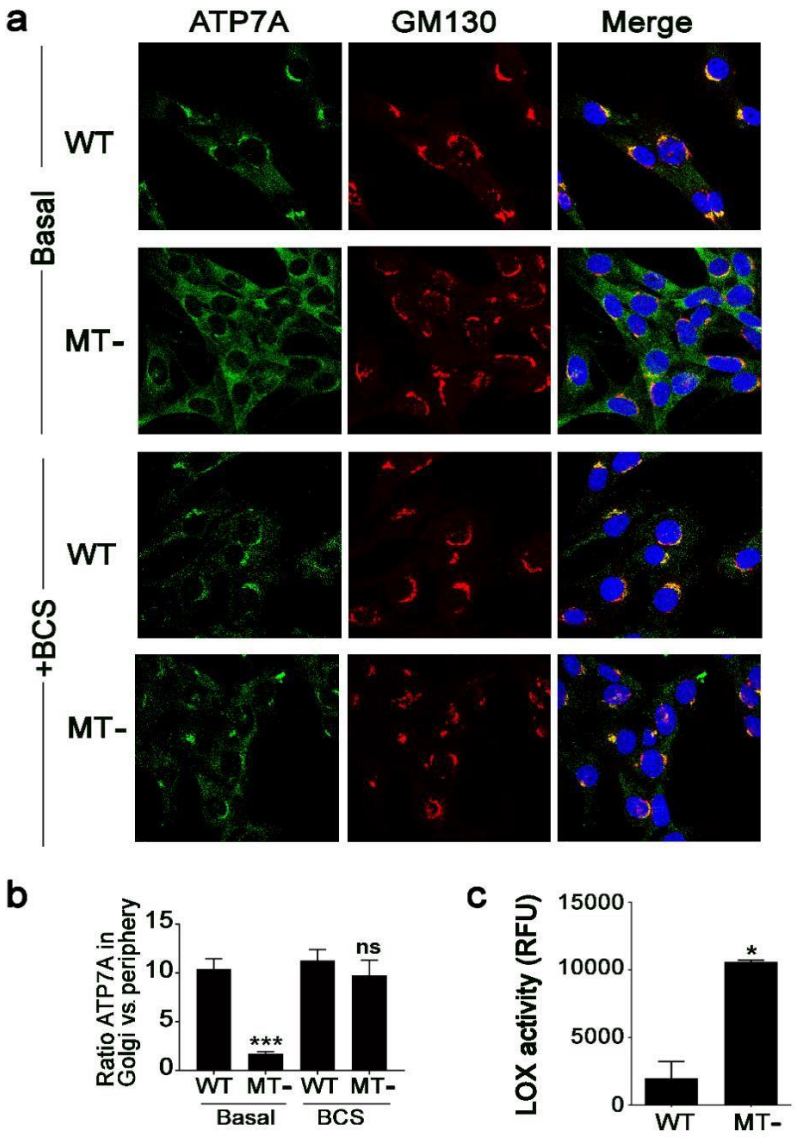
a
ATP7A
GM130
Merge
WT
MT-
Basal
+BCS
b
Ratio ATP7A in Golgi vs periphery
15
10
5
0
***
ns
WT
MT-
WT
MT-
Basal
BCS
c
LOX activity (RFU)
15000
10000
5000
0
*
WT
MT-

Fig. II-6: ATP7A and MTs decrease cell viability during Cu starvation. (**a**) WT, ATP7A-, MT- and ATP7A-/MT- cells were seeded into 6-well plates (2 x 10^4 cells/well) and cultured in medium supplemented with 50 µM BCS. After 4 days, cells were stained with Crystal Violet and imaged. (**b**) A second batch of identically treated cells was passaged for an additional 4 days in BCS-containing medium and then stained with Crystal Violet (*i.e.*, after 8 days of Cu chelation). Crystal Violet staining in both (**a**) and (**b**) was quantified as a measure of cell survival. Values were normalized against the survival of the ATP7A-/MT- cell line in BCS at Day 4 and Day 8 (mean ± SEM). Different letters indicate values that are significantly different from each other. Note that the loss of ATP7A or MTI/II enhances the ability of cells to propagate in the presence of the BCS copper chelator.

Fig. II-6

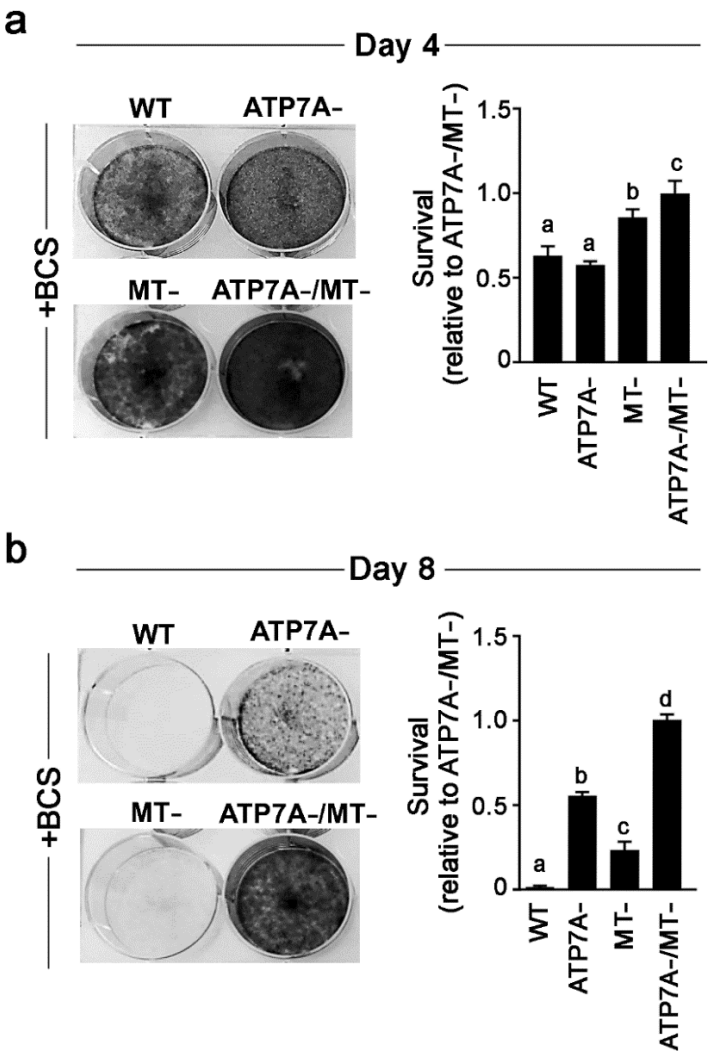
a
Day 4
WT
ATP7A-
+BCS
MT-
ATP7A-/MT-
Survival
(relative to ATP7A-/MT-)
1.5
1.0
0.5
0
a
a
b
c
WT
ATP7A-
MT-
ATP7A-/MT-
b
Day 8
WT
ATP7A-
+BCS
MT-
ATP7A-/MT-
Survival
(relative to ATP7A-/MT-)
1.5
1.0
0.5
0
a
b
c
d
WT
ATP7A-
MT-
ATP7A-/MT-

Supplementary information

Fig. II-S1: Breeding strategy used to generate *Atp7a* floxed mice carrying deletions in *Mtl* and *Mtll* genes. The *Mtl/II* knockout mice were crossed with *Atp7a* floxed mice to produce F1 offspring that were heterozygous at the *Mtl/II* locus and either Wt or floxed at the *Atp7a* locus. These mice were crossed to produce male *Atp7a* floxed mice that were homozygous null for the *Mtl/II* alleles.

Fig. II-S1

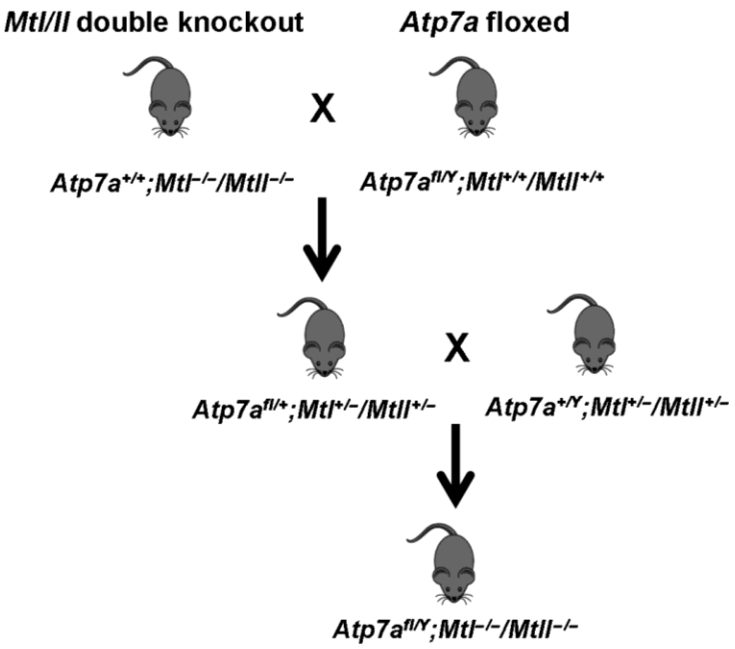
Mtl/II double knockout
Atp7a floxed
X
$Atp7a^{+/+};Mtl^{-/-}/Mtll^{-/-}$
$Atp7a^{fl/Y};Mtl^{+/+}/Mtll^{+/+}$
$Atp7a^{fl/+};Mtl^{+/-}/Mtll^{+/-}$
X
$Atp7a^{+/Y};Mtl^{+/-}/Mtll^{+/-}$
$Atp7a^{fl/Y};Mtl^{-/-}/Mtll^{-/-}$

Fig. II-S2: Deletion of the *Atp7a* gene in MT- cells causes a loss of cell viability that is rescued by Cu chelation. MT- cells were seeded overnight in basal medium at approximately 30% confluency (top panel), infected with an adenoviral Cre vector to delete the *Atp7a* gene and then cultured for 5 days in basal media with or without 50 µM BCS (bottom panels). Images were collected by light microscopy; bars, 50 µm.

Fig. II-S2

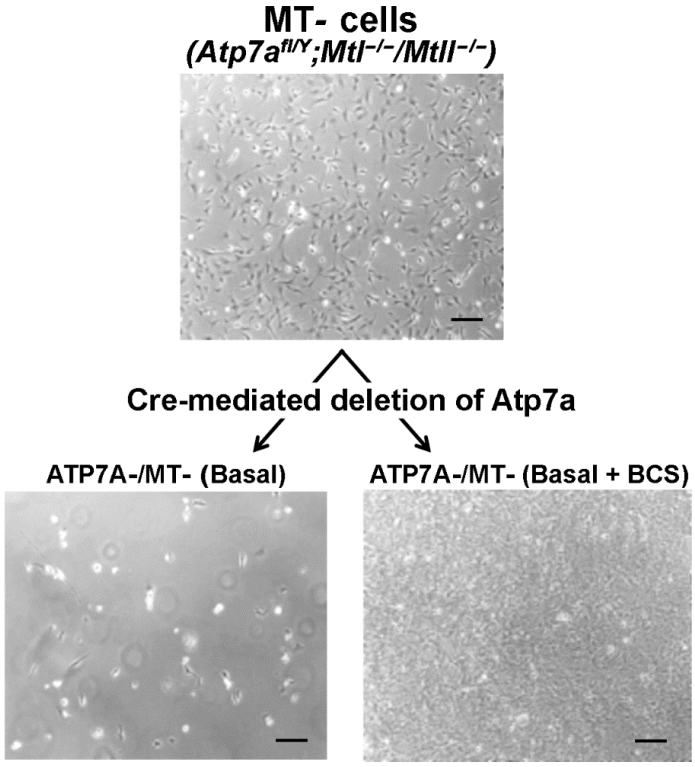
MT- cells
(Atp7a^fl/Y;Mtl^-/-/Mtll^-/-)
Cre-mediated deletion of Atp7a
ATP7A-/MT- (Basal)
ATP7A-/MT- (Basal + BCS)

Fig. II-S3: Iron (Fe) and Zinc (Zn) concentrations in each cell line were determined by ICP-MS. Cells were grown for 2 days in medium containing 50 µM of the copper chelator BCS and then exposed for 24 h to either basal media (basal) or media supplemented with 50 µM BCS and levels of (**a and b**) Fe or (**c and d**) Zn were measured. Values significantly different from WT are indicated (mean ± SEM; *p < 0.05; **p < 0.01; ***p < 0.001; ns = not significant).

Fig. II-S3

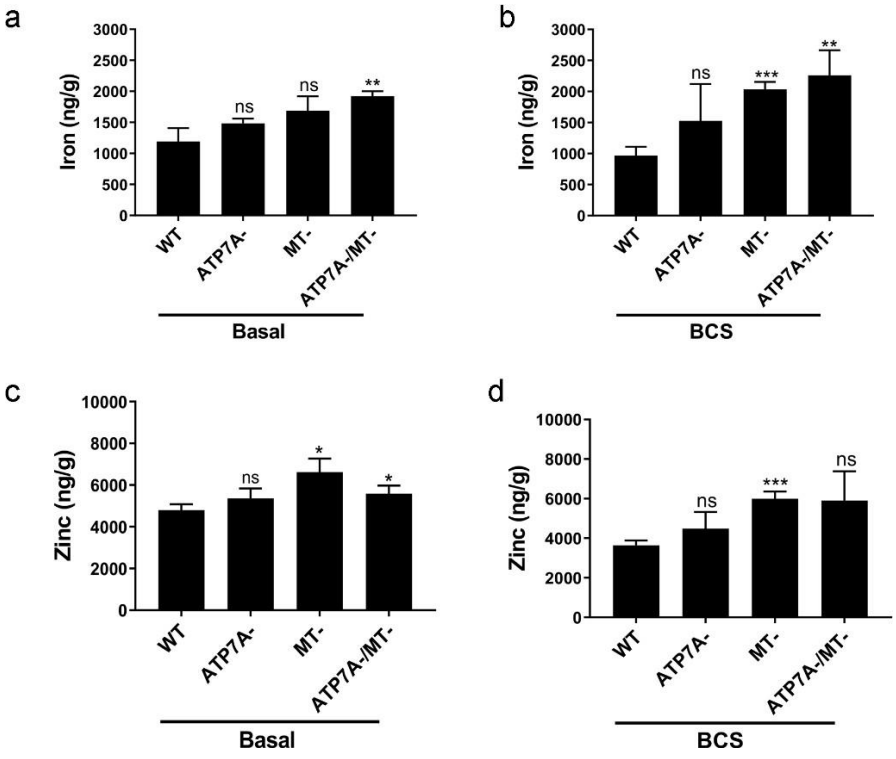
a
b
c
d
Iron (ng/g)
Zinc (ng/g)
3000
2500
2000
1500
1000
500
0
10000
8000
6000
4000
2000
ns
*
**
***
WT
ATP7A-
MT-
ATP7A-/MT-
Basal
BCS

Fig. II-S4: Deletion of *ATP7A* and *MTI/II* causes hypersensitivity to sub-micromolar Cu concentrations. ATP7A-/MT- cells were seeded into 6-well dishes (10^3 cells per well) and cultured for 6 days in media supplemented with 1 μM BCS with or without the indicated concentrations of $CuCl_2$. Surviving cells were quantified using the Crystal Violet assay (mean ± SEM).

Fig. II-S4

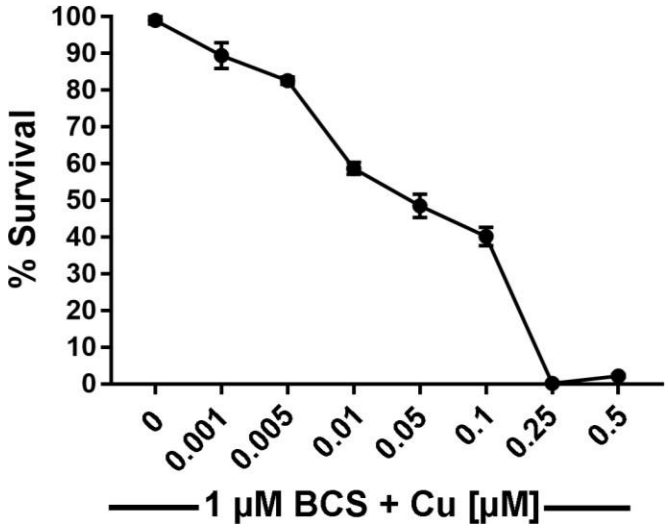
% Survival
100
90
80
70
60
50
40
30
20
10
0
0
0.001
0.005
0.01
0.05
0.1
0.25
0.5
1 µM BCS + Cu [µM]

Fig. II-S5: Deletion of *ATP7A* and *MTI/II* increases cellular GSH levels and reduces the ratio of reduced glutathione (GSH) to oxidized glutathione (GSSG). Cellular GSH per mg total protein (**a**) and the GSH/GSSG ratio (**b**) were measured in wild type (127) and mutant cells cultured for 24 h in basal medium. Values are expressed as the mean ± SEM (*$p < 0.05$; ***$p < 0.001$; ****$p < 0.0001$; $n = 3$).

Fig. II-S5

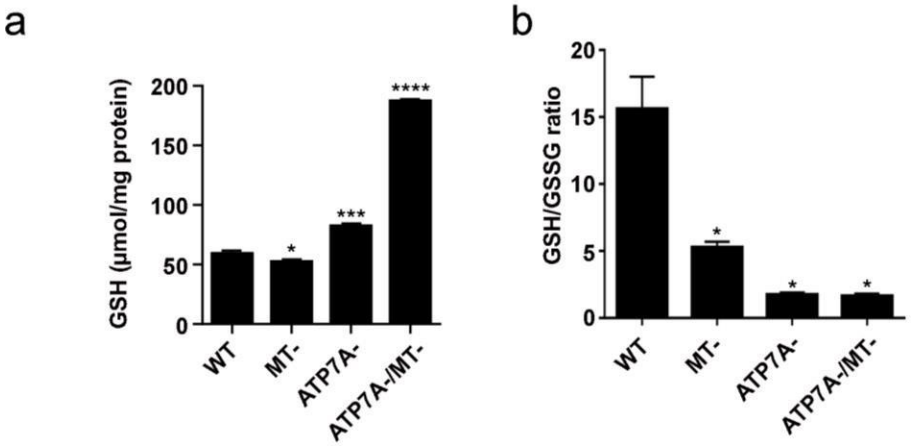
a
GSH (µmol/mg protein)
200
150
100
50
0
*
***
****
WT
MT-
ATP7A-
ATP7A-/MT-
b
GSH/GSSG ratio
20
15
10
5
0
*
*
*
WT
MT-
ATP7A-
ATP7A-/MT-

Fig. II-S6: Quantitative real time PCR analysis of *Atp7a* and *Atp7b* mRNA expression in spontaneously Cu resistant cell lines. (**a**) Parental ATP7A-/MT- (control) cells were selected in either basal medium (basal) or 20 µM $CuCl_2$ (CuR20). Quantitative real time PCR was used to measure the abundance of *Atp7b* mRNA in each line normalized to *Gapdh* (mean ± SEM; ****p < 0.0001; n = 3). (**b and c**) Parental ATP7A+/MT- cells were grown in either basal medium (basal) or passaged in media containing elevated $CuCl_2$ until resistance to 900 µM Cu was achieved (CuR900). Quantitative real time PCR was used to measure the abundance of *Atp7a* and *Atp7b* mRNA in each line normalized to *Gapdh* (mean ± SEM; ****p < 0.0001; n = 3).

Fig. II-S6

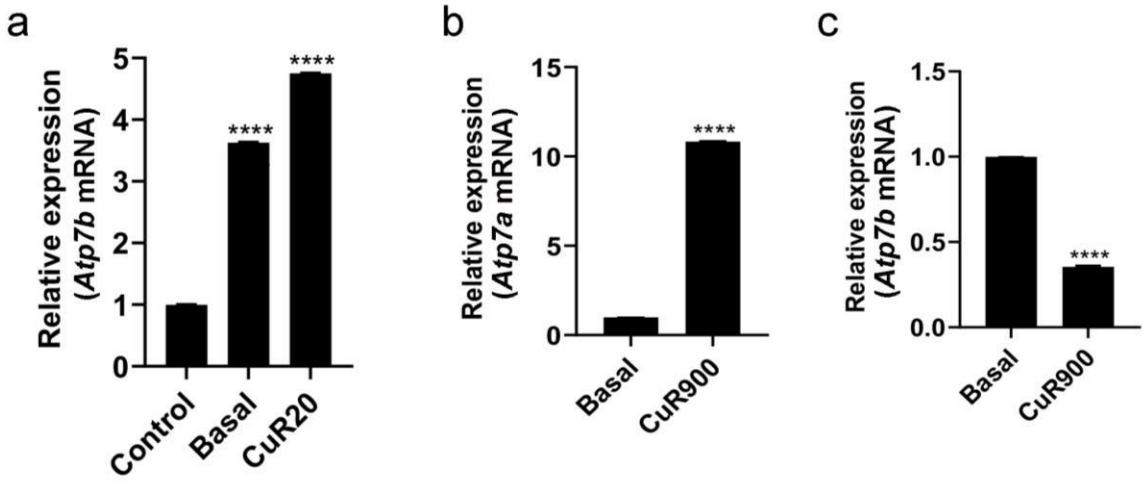
a
Relative expression (*Atp7b* mRNA)
5
4
3
2
1
0
****
****
Control
Basal
CuR20
b
Relative expression (*Atp7a* mRNA)
15
10
5
0
****
Basal
CuR900
c
Relative expression (*Atp7b* mRNA)
1.5
1.0
0.5
0.0
****
Basal
CuR900

Fig. II-S7 Full length gels and immunoblot from Figure 1

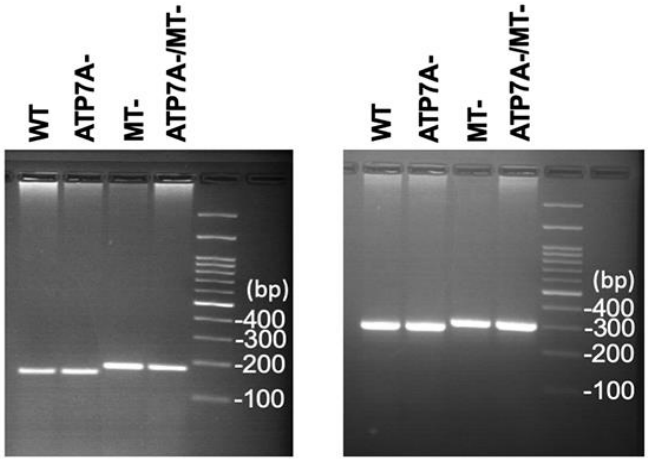

Fig. 1b

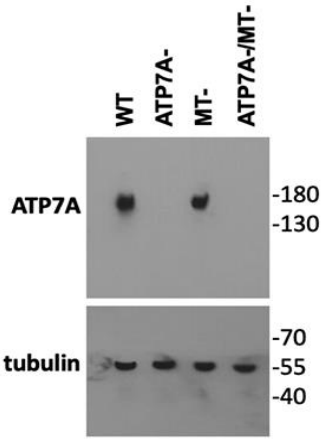

Fig. 1c

Fig. II-S8 Full length gels and immunoblot from Figure 4

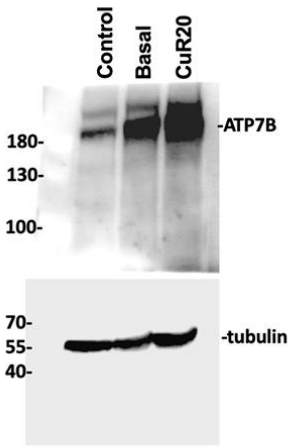

Fig. 4a

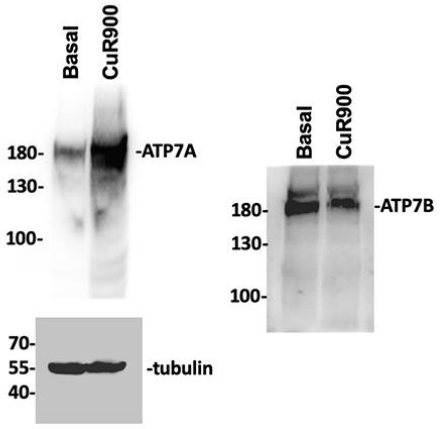

Fig. 4c

Chapter III

VHL-mediated regulation of ATP7B connects oxygen and copper metabolism

Statement of Contributions: I designed and performed the majority of the experiments, including in Figures 1 to 4.

Abstract

Copper (Cu) is an essential trace dietary metal which is also potentially toxic. Cells have evolved an intricate system of transporters and chaperones to carefully regulate Cu homeostasis. Previously, we generated a fibroblast cell line in which genes encoding the copper transporter, *Atp7a*, and copper-binding proteins, metallothioneins I and II (*Mt-I* and *Mt-II*) were deleted. This resulted in a copper sensitive cell line (Cu^S) that was sensitive to sub-micromolar levels of copper. Using a genome-wide CRISPR-Cas9 deletion screen, we identified a novel gene, *Vhl* (von Hippel-Lindau), that when deleted confers Cu tolerance to the Cu^S cells. The VHL protein is a part of the ubiquitin-ligase complex responsible for the degradation of HIF transcription factors, which are the major regulators of gene expression in response to hypoxia. We show that VHL deletion confers Cu tolerance by stimulating the expression of the ATP7B copper transporter. Pharmacological inhibition of VHL-HIF1α by Roxadustat (a prolyl hydroxylase inhibitor), conferred resistance to copper by upregulating ATP7B. Importantly, hypoxia or Roxadustat treatment enhanced hepatic ATP7B expression *in vivo*. These novel data identify a previously unknown link between copper homeostasis and oxygen sensing with translational implications for the treatment of Wilson disease, a copper overload condition caused by insufficient expression of ATP7B.

3.1 Introduction

Copper (Cu) is an enzymatic cofactor required for cellular respiration, melanogenesis, neurotransmitter biosynthesis and connective tissue formation (2). The requirement for Cu lies in its ability to cycle between Cu(I) and Cu(II) oxidation states; however, this redox property also underlies copper's toxicity if concentrations become elevated. The dichotomy of Cu as an essential yet potentially toxic nutrient is illustrated by two diseases of Cu metabolism, Menkes and Wilson diseases. Menkes disease is a disorder of Cu deficiency caused by mutations in the ATP7A Cu transporter (73). In contrast, Wilson disease is a disorder of Cu overload caused by mutations in the ATP7B Cu transporter (132).

It is remarkable that virtually all genes known to regulate Cu homeostasis in mammalian cells were initially cloned in the single-cell microbe, *Saccharomyces cerevisiae*. While this clearly demonstrates that many Cu handling pathways are highly conserved in all eukaryotes, it also suggests that there may be undiscovered mechanisms of copper homeostasis unique to complex multicellular eukaryotes.

Recent advances in gene targeting technology, such as CRISPR, offer new opportunities to clone such genes. In this study, we started with a cell line that is highly sensitive to copper (Cu^S cells) that were generated by a triple knockout of

ATP7A and the metallothioneins, MTI and MTII. Next, we used the Cu^S cells in a genome-wide CRISPR-based deletion screen to identify novel genes that when disrupted confer Cu tolerance. Using this strategy, we demonstrated that deletion of von Hippel-Lindau (VHL) protein in Cu^S cells results in a massive upregulation of the ATP7B copper exporter, which confers tolerance to copper. VHL is part of a ubiquitin-ligase complex that ubiquitylates target proteins, marking them for proteasomal degradation (133). In work recognized by the 2019 Nobel Prize for Medicine, the most well characterized function of VHL is the targeted degradation of the transcription factors, HIF1α and HIF2α. Under normoxic conditions, VHL protein together with oxygen-dependent prolyl hydroxylases (PHDs) facilitate the degradation of HIF1α and HIF2α (134). Under hypoxic conditions, the lack of oxygen suppresses the ability of PHDs to hydroxylate HIF1α, resulting in increased levels of HIF1α that allows it to heterodimerize with HIF1β and enter the nucleus. This complex then drives a myriad of target genes through binding to hypoxia response elements present in their promoter regions (133-135). Known HIF target genes include metabolic genes required for adaptation to low oxygen conditions, including genes involved in glucose uptake, glycolysis, iron acquisition and heme synthesis.

Here, we demonstrate for the first time that genetic disruption of VHL or pharmacological inhibition of the VHL-PHD pathway results in upregulation of ATP7B expression in cultured cells, suggesting that ATP7B is a novel target of HIF1. Consistent with these observations, pharmacological inhibition of the

VHL-PHD pathway in mice or exposure to hypoxia resulted in marked increases in ATP7B abundance in liver. These findings reveal an unexpected interplay between copper metabolism and oxygen sensing and suggest that VHL-PHD inhibitors could be repurposed to treat diseases of ATP7B deficiency.

3.2 Results

3.2.1 Genome-wide CRISPR-based screen for Cu tolerance in Cu^{s} cells.

Previously, we discovered that the Cu^{S} cells were completely inviable when seeded into Dulbecco's Modified Eagle's medium (hereafter called basal medium; ~1.7 µM Cu). However, these cells could be propagated indefinitely in basal medium containing the cell-impermeable Cu chelator, bathocuproine disulfonate (BCS) (as described in Chapter II). Thus, having successfully generated an innovative cell line that is exquisitely sensitive to Cu, we proceeded with a CRISPR-based deletion screen to identify regulators of Cu tolerance.

A lentiviral CRISPR library (GeCKOv2; Addgene 50947) containing ~130,000 guide RNAs (gRNAs) directed against approximately 20,000 genes was used to infect the Cu^{S} cells. A control pool of stably transduced cells was selected for 10 days in BCS-containing medium supplemented with puromycin, because the CRISPR library plasmids had puromycin selectable marker. Next, a Cu- tolerant

pool of cells was obtained by culturing half of the control pool for a further 10 days in BCS-free medium containing puromycin and 1 µM $CuCl_2$.

Genomic DNA was purified from both the control and Cu-tolerant pools and the integrated gRNAs were amplified by PCR and then subjected to identification and quantification using next generation sequencing (Fig. III-1A). The Illumina sequencing data was obtained from the University of Missouri DNA Core Facility The Post-sequencing processing was performed by the MU Informatics Research Core Facility Next generation sequencing. The FASTQ files obtained from the sequencing data were then analyzed using the Tuxedo pipeline workflow. Candidate gRNAs responsible for conferring Cu tolerance were identified by calculating their abundance in the Cu tolerant pool relative to the control pool. Using this approach, we identified three gRNAs against the copper importer, CTR1, that were most enriched by Cu selection (Supplementary Fig. III-S1A), suggesting that disruption of CTR1 confers Cu tolerance in Cu^S cells. This was confirmed in a separate experiment by showing that two different gRNA constructs against CTR1 that were not present in the library (Supplementary Fig. III-S1B) also conferred Cu tolerance when stably transfected into Cu^S cells. Single colonies were picked to generate clonally pure Cu^S/CTR1- cell lines. The Cu resistance profile of the Cu^S/CTR1- cell line is shown (Fig. III-1B). Sequence analysis of one of these cell lines confirmed the insertion of a single nucleotide in the open reading frame of the *Ctr1* gene (Fig. III-1C). Our sequence analysis revealed that the second most enriched group of gRNAs was against the von Hippel Lindau (*Vhl*) gene (Supplementary Fig. III-S1A), which has no previously

defined role in Cu tolerance. We confirmed this finding by targeting *Vhl* using a CRISPR gRNA. DNA sequence analysis confirmed a two-nucleotide deletion in *Vhl* (Fig. III-1D). As with CTR1, we demonstrated that two different gRNAs against the *Vhl* gene that were not present in the original library (Supplementary Fig. III-S1B) also conferred Cu tolerance in Cu^S cells. The Cu resistance profile of one clonally derived Cu^S/VHL- cell line is shown (Fig. III-1B).

3.2.2 Disruption of the *Vhl* gene in Cu^S cells confers Cu tolerance by stimulating expression of the ATP7B protein

Our next objective was to identify the underlying mechanism of copper tolerance in Cu^S/VHL- cells. Previous studies have shown that forced expression of ATP7B can increase Cu tolerance in cells lacking ATP7A (115, 116). Thus, we hypothesized that elevated expression of ATP7B might account for the increased Cu tolerance in the Cu^S/VHL- cells. Consistent with our hypothesis, we found that ATP7B expression was elevated at the level of protein and mRNA in Cu^S/VHL- cells, compared to control Cu^S cells (Figs. III-2A and III-2B). Using immunofluorescence microscopy, we detected a very weak signal in control Cu^S cells using anti-ATP7B antibodies. However, in the Cu^S/VHL- cells, we detected a strong signal in the perinuclear region, consistent with the Golgi localization of ATP7B (Fig. III-2C). Consistent with this finding, we also found a significant upregulation of *Atp7b* mRNA in a *Vhl* knockout Renca cell-line (Renca *Vhl*-) (Figs. III-2D and 2E). Complementation of Cu^S/VHL- cells by transient

transfection with an HA-tagged VHL expression plasmid resulted in the loss of ATP7B staining in the perinuclear region of VHL-HA positive cells (Fig. III-2F, asterisk). However, the loss of ATP7B did not occur in neighboring cells that failed to express the plasmid (Fig. III-2F, arrows). In additional experiments, we found that stable transfection of Cu^S cells with an ATP7B expression plasmid was sufficient to confer Cu tolerance (Figs. III-2G and III-2H), which confirmed that the increased expression of ATP7B confers Cu tolerance in Cu^S/VHL- cells.

Taken together, these results demonstrate that disruption of the *Vhl* gene confers Cu tolerance due to upregulation of ATP7B expression.

3.2.3 Pharmacological inhibition of prolyl hydroxylases stimulates expression of the ATP7B protein

Previous studies have demonstrated that a key target of VHL is the HIF transcription factor (Fig. III-3A). The mechanism by which HIF1/2α is degraded under normal oxygen conditions involves a two-step process that includes: 1) hydroxylation of key proline by prolyl hydroxylase domain (PHD) proteins that require iron (Fe) and molecular oxygen for this process; and 2) ubiquitination of HIF1/2α by VHL that targets it for proteasomal degradation (Fig. III-3A) (136). Our working model at this stage was that ATP7B expression is induced by HIF-mediated transcription and is therefore subject to control by VHL/PHD-mediated HIF degradation (Fig. III-3A). A prediction of this model is that a PHD protein inhibitor should increase the expression of ATP7B and confer increased Cu

tolerance to Cu^S cells. Consistent with our hypothesis, Cu^S cells were found to propagate in basal medium containing Roxadustat, which is a clinically approved inhibitor of PHD proteins (Fig. III-3B). Importantly, Roxadustat was found to stimulate expression of *Atp7b* mRNA and protein in Cu^S cells (Figs. III-3C, III-3D and IIIE). To validate whether Roxadustat-induced ATP7B expression occurs *in vivo*, we administered Roxadustat (10 mg/kg) to 8-week-old C57BL/6 mice via intraperitoneal injection. Total membrane preparations were obtained from liver homogenates (MemPer kit, ThermoFisher) and subjected to SDS-PAGE and immunoblot analysis. ATP7B protein abundance was found to be markedly elevated in the liver of all mice treated with Roxadustat compared to mice treated with vehicle control (Fig. III-3F). Taken together, our data indicate that *Atp7b* gene expression is induced by the PHD protein inhibitor Roxadustat and targeted disruption of the *Vhl* gene, suggesting *Atp7b* may be a HIF target.

3.2.4 Hypoxia stimulates expression of the ATP7B protein in mice

Another regulator of the VHL/PHD/HIF pathway is low oxygen (hypoxia). Because VHL deletion mimics the effects of hypoxia, we assessed the effect of hypoxic conditions on the upregulation of ATP7B and the survival of Cu^S cells in the presence of copper. Cu^S cells were grown in basal or BCS-containing media under hypoxic or normoxic conditions. It was observed that hypoxia was able to rescue Cu^S cells grown in basal media (Fig. III-4A).

To test if this survival was due to upregulation of ATP7B in these cells, we determined the mRNA levels of *Atp7b* in Cu^S cells grown under hypoxia and normoxia and significant upregulation of *Atp7b* mRNA was observed under hypoxic conditions (Fig. III-4B). To further test whether hypoxia stimulates ATP7B protein expression *in vivo*, we exposed wild type C57BL/6 mice (age 8 weeks) to normoxia (21% O_2) or hypoxia (6% O_2). As described above, ATP7B protein was detected in the livers of mice. ATP7B expression was found to be significantly upregulated in livers obtained from mice exposed to hypoxia, as compared to normoxia (Fig. III-4C). Taken together, these results demonstrate that the *Atp7b* gene is likely a HIF target and suggest that oxygen limitation induces increases in ATP7B-dependent Cu transport.

3.3 Discussion

A low level of molecular oxygen or hypoxia is a normal physiological stress and, importantly, hypoxia contributes to the pathogenesis of many common diseases. Understanding the mechanisms that regulate adaptations to hypoxia are of fundamental importance to physiology and medicine (137). Because the capacity to carry oxygen in red blood cells is dependent on iron (Fe) within hemoglobin, an important adaptation to hypoxia is to increase iron export from enterocytes, hepatocytes and macrophages into the plasma. Iron is essential for oxygen transport in the blood as a component of heme. The availability of iron for erythropoiesis is regulated in part by the hormone hepcidin, which binds to

ferroportin and triggers its internalization and degradation. Hepcidin production is suppressed under conditions of high erythropoietic demand, thus ensuring a greater capacity for ferroportin-mediated iron export into the plasma (138, 139). Another hormone, erythropoietin (EPO) is induced in response to hypoxia mainly in the kidney and stimulates erythropoiesis in the bone marrow. In addition, hypoxia stimulates the expression of multiple proteins involved in iron homeostasis including ferroportin, transferrin, transferrin receptor, heme oxygenase and ceruloplasmin. Collectively, these proteins increase iron absorption and release from stores to meet the increased iron demand for erythropoiesis (140).

The copper-dependent ferroxidase, ceruloplasmin, plays an important role in this adaptive response by converting Fe^{2+} to Fe^{3+}, and in doing so facilitates iron export via the iron exporter, ferroportin, and the subsequent loading of Fe^{3+} onto transferrin. Ceruloplasmin must acquire copper during its maturation within the secretory pathway, a process that is mediated by the Golgi-localized copper transporter, ATP7B (141, 142). Ceruloplasmin is secreted from hepatocytes into the plasma and facilitates iron export from the liver and macrophages. While ceruloplasmin illustrates the importance of copper for iron export, remarkably little is known regarding the relationship between oxygen availability and copper homeostasis.

Using a genetic screen for copper tolerance, we demonstrate that ATP7B expression is strongly induced by deleting the von Hippel Lindau (*Vhl*) gene. Upregulation of ATP7B upon ablation of *Vhl* was also observed in other *Vhl*-null cell lines (Fig III-2E). VHL is a master regulator of oxygen sensing machinery and the best-known function of VHL is to regulate the hypoxia response genes known as hypoxia inducible factors (HIF1α and HIF2α). Under normal oxygen conditions, VHL along with prolyl hydroxylase domain (PHD) proteins target HIFs for degradation (143). The PHDs hydroxylate the proline residues present in the LXXLAP motif of HIF proteins. The PHDs are oxygen and 2-oxoglutarate dependent oxygenases that require Fe^{2+} as cofactor for their catalytic activity (144). Hydroxylation of a proline residue is most common post translational modification typically known to be involved in providing structural stability to a protein. The hydroxylation of specific proline residues in collagen is required for the stability of collagen triple helix (145,146). This process is carried out by collagen prolyl hydroxylases (C-P4Hs) that belong to the same superfamily of proteins as the HIF-prolyl hydroxylases (HIF-PHDs) sharing common enzymatic mechanism (146,147). While the HIF-PHDs can specifically bind to the proline residues in the conserved LXXLAP of HIF proteins, the C-P4Hs are specific to collagen binding domain (-X-Pro-Gly) and cannot hydroxylate the conserved proline residue present in the HIF proteins (148,149). Post translational modification is also involved in cellular signaling, as evidenced by the initiation of the hypoxic response by the HIF transcription factors upon hydroxylation by the HIF-PHDs. Of the three well known isoforms of PHDs, PHD2 is considered

to be the most important sensor of the oxygen status in the cells. Thus, we previously tested whether the deletion of PHD2 using CRISPR Cas9 system allows the survival of the Cu^S cells. Three different gRNAs directed against PHD2 gene were ordered from genecopeia (MCP237008-SG01-3-10-a, MCP237008-SG01-3-10-b and MCP237008-SG01-3-10-c) and tested on Cu^S cells. The CRISPR-Cas9 treatment did not allow the survival of these cells in basal media suggesting a functional redundancy in the PHDs.

Thus, pharmacological inhibition of the PHDs is efficient way to stabilize HIF proteins. Roxadustat, a specific inhibitor of PHD proteins, used to treat patients with certain types of anemia by stimulating the expression of HIF-target genes (e.g., erythropoietin), resulting in improved red cell counts and increased iron absorption (150). Pharmacological inhibition of PHD proteins using Roxadustat, in both cultured cells and mice resulted in a significant upregulation of the expression of ATP7B (mRNA and protein) (Figs. III-3C, III-3D and III-3E). More importantly, we demonstrate that Roxadustat (Fig. III-3F) and hypoxia (Fig. III-4C) upregulate the hepatic expression of ATP7B. We propose that upregulation of hepatic ATP7B under hypoxic conditions may provide a means for increased copper transport and activity of ceruloplasmin, enabling higher iron export to meet the urgent demand for iron in the process of erythropoiesis.

Thus, our novel discovery connects oxygen, iron and copper homeostasis and

could possibly provide a mechanistic link for the adaptive responses occurring during hypoxia.

3.4 Experimental procedures

Tissue culture

Cells were cultured in Dulbecco's modified Eagle's medium (Life Technologies) containing 10% (v/v) fetal bovine serum, 100 U/ml penicillin and streptomycin, 100 U/ml L-glutamine and 100 U/ml non-essential amino acids (Life Technologies) at 37ºC in an atmosphere of 5% CO_2. The Cu^S cell line was obtained, as described previously (33).

Protein expression and localization

Immunoblot analysis: Cells were scraped directly into lysis buffer (PBS containing 2% (w/v) SDS, 1 mM EDTA, 1% (v/v) Triton X-100, 62.5 mM Tris) and protease inhibitor mixture (Sigma Aldrich). Samples were fractionated by SDS-PAGE using a mini-PROTEAN 3 gel unit (Bio-rad). Proteins were detected using rabbit anti-ATP7B (1:500) (33) and mouse anti-tubulin (1:2000) (Sigma Aldrich) primary antibodies followed by secondary antibody conjugated to HRP (horseradish peroxidase) from Sigma Aldrich (horseradish peroxidase-conjugated anti-rabbit IgG; Santa Cruz SC2357, anti-mouse IgG; ThermoFisher 31430) at 1:1000 dilution. Nitrocellulose membranes were maintained in 1%

(w/v) bovine serum albumin (BSA) in 1X TBST (0.1% Tween -20 dissolved in 1X TBS) until the very last step. Molecular weight markers used were PageRuler (#26616 ThermoFisher).

Immunofluorescence microscopy: Cells were cultured in 6 well dishes on sterile coverslips. The cells were fixed using 4% (v/v) paraformaldehyde (PFA) followed by 0.1% (v/v) Triton X-100. The cells were blocked using 1% BSA (prepared in 1X PBS). Primary antibody was used for immunostaining of ATP7B. Cells were then probed with secondary antibody, Alexa Fluor 488-conjugated anti-rabbit IgG (ThermoFisher; A11034). For nuclei staining, DAPI (4',6 diamidino-2-phenylindole) was used and cells were imaged using a Leica DMRE fluorescence microscope.

Plasmids

Plasmid expressing *Atp7b* was transfected in Cu^S cells using Lipofectamine 2000 (Invitrogen) and selected in basal medium supplemented with 1 µM $CuCl_2$. Surviving colonies were expanded and immunoblot analysis was performed to detect ATP7B. CRISPR-Cas9 plasmids targeting *Ctr1*: gRNA 5'-GGACTCAAGATAGCCCGAGAGG and *Vhl*: gRNA 5'-GAACTCGCGCGAGCCCTCTC were ordered from Sigma Aldrich and Genecopeia, respectively.

Cell viability analysis

Cell survival was measured using the Crystal Violet assay, as described previously (129).

RNA isolation and quantitative real time PCR (qPCR)

RNA was purified using the RNeasy Plus kit (Qiagen, 74134) and cDNA was synthesized using the RNA to cDNA EcoDry kit (Takara), according to the manufacturer's instructions. Quantitative real time PCR analysis was performed using Taqman probes from Applied Biosystems for *Atp7b* (Mm00599675), *Vhl* (Mm00494137) and *S18* (4333760T).

Animals

All animal husbandry and euthanasia procedures were performed with the approval of the University of Missouri's Animal Care and Use Committee. A hypoxic chamber was engineered to provide highly controlled oxygen environment for mice models. The chamber was connected to a nitrogen tank to displace air in the chamber to achieve 6% O_2 throughout the experiment. Mice were maintained under these hypoxic conditions for five days.

Statistical analyses

Statistical analyses were performed using GraphPad Prism 7.0. Data are presented as mean ± SEM (standard error of the mean) of at least three biological replicates. Data were analyzed using the standard Student's t-test (statistical significance when $p < 0.05$). Statistical significance representations: ****$p < 0.0001$.

3.5 Figures

Fig. III-1: A genome-wide knockout screen identifies the von Hippel Lindau (*Vhl*) gene as a novel regulator of Cu tolerance. (**A**) Workflow of our CRISPR-based screen to identify gRNAs that confer Cu tolerance in Cu^S cells. (**B**) Secondary validation of library hits using the Crystal Violet cell survival assay. Cu^S cells were transfected with gRNAs against *Ctr1* and *Vhl*, and then selected for 10 days in medium containing puromycin plus 1 µM $CuCl_2$. Colonies were picked and expanded to derive Cu^S/CTR1- and Cu^S/VHL- cell lines. The degree of Cu resistance was determined using the Crystal Violet assay. Cell lines were seeded into six well plates (10^3 cells /well) with or without the indicated concentrations of BCS or Cu. After 5 days, colonies were stained with Crystal Violet and imaged. (**C and D**) Single colonies were picked to generate clonally pure Cu^S/CTR1- and Cu^S/VHL- cell lines. Genomic DNA was isolated from Cu^S, Cu^S/CTR1- and Cu^S/VHL- cells and PCR was performed using specific primers.

Fig. III-1

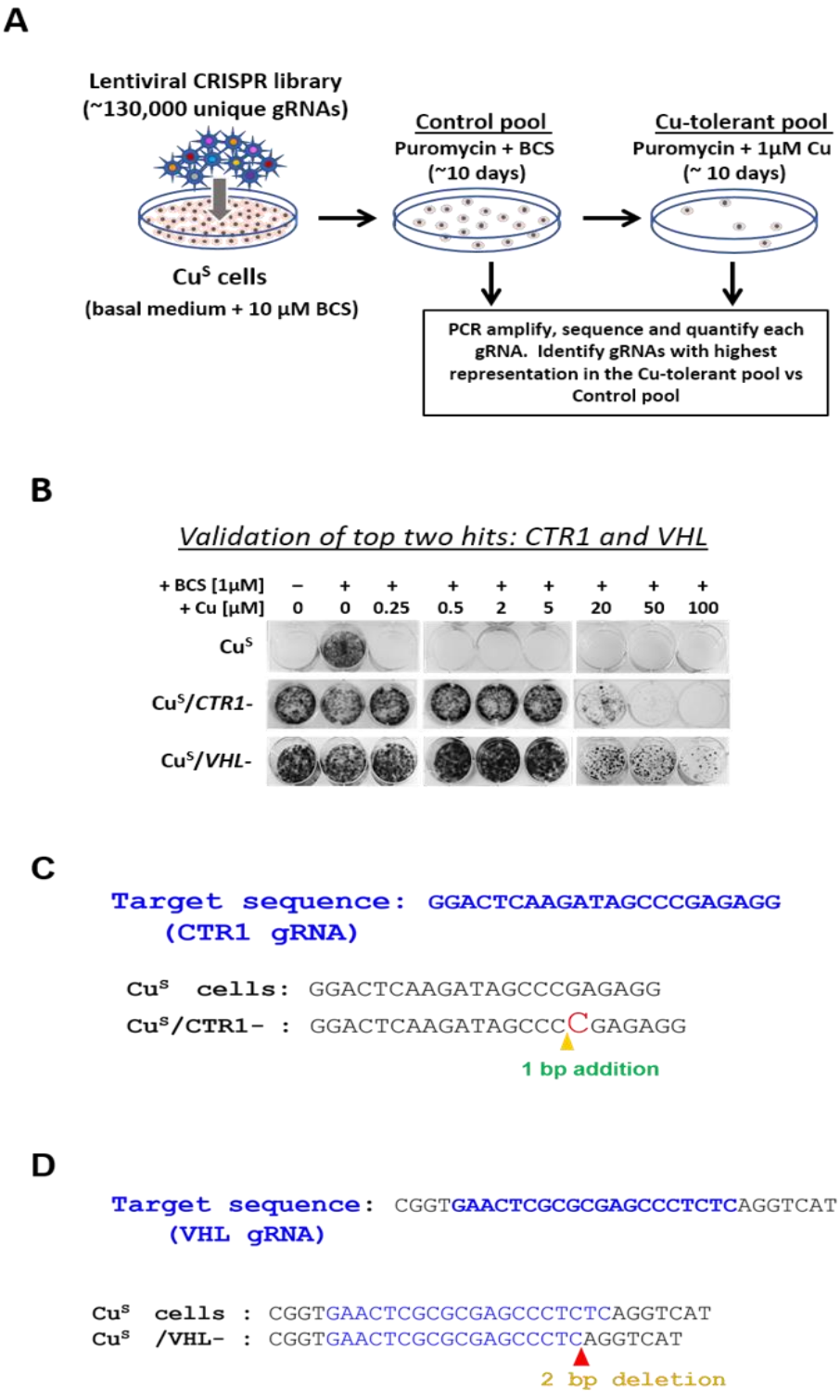
A
Lentiviral CRISPR library
(~130,000 unique gRNAs)
Cu^S cells
(basal medium + 10 µM BCS)
Control pool
Puromycin + BCS
(~10 days)
Cu-tolerant pool
Puromycin + 1µM Cu
(~ 10 days)
PCR amplify, sequence and quantify each gRNA. Identify gRNAs with highest representation in the Cu-tolerant pool vs Control pool
B
Validation of top two hits: CTR1 and VHL
+ BCS [1µM] – + + + + + + + +
+ Cu [µM] 0 0 0.25 0.5 2 5 20 50 100
Cu^S
Cu^S/CTR1-
Cu^S/VHL-
C
Target sequence: GGACTCAAGATAGCCCGAGAGG
(CTR1 gRNA)
Cu^S cells: GGACTCAAGATAGCCCGAGAGG
Cu^S/CTR1- : GGACTCAAGATAGCCCCGAGAGG
1 bp addition
D
Target sequence: CGGTGAACTCGCGCGAGCCCTCTCAGGTCAT
(VHL gRNA)
Cu^S cells : CGGTGAACTCGCGCGAGCCCTCTCAGGTCAT
Cu^S /VHL- : CGGTGAACTCGCGCGAGCCCTCAGGTCAT
2 bp deletion

Fig. III-2: CRISPR-targeted disruption of the *Vhl* gene induces ATP7B expression at the mRNA and protein level. (**A**) Cu^S cells were stably transfected with a CRISPR construct containing a gRNA against *Vhl* to generate Cu^S/VHL-. Immunoblot analysis was performed to detect ATP7B and HIF1α in Cu^S/VHL- cells, compared to the parental Cu^S cells. (**B**) Quantitative real time PCR was performed to detect *Atp7b* mRNA levels in Cu^S/VHL- cells. Values are expressed as the mean ± SEM (****$p < 0.0001$; $n = 3$). (**C**) Immunofluorescence microscopy was performed to detect ATP7B protein (green) upon deletion of VHL. Nuclei were stained with DAPI (blue). (**D and E**) Quantitative real time PCR was performed to detect *Vhl* and *Atp7b* mRNA levels in Renca and Renca *Vhl*- cells. Values are expressed as the mean ± SEM (****$p < 0.0001$; $n = 3$). (**F**) Cu^S/VHL- cells were transiently transfected with VHL plasmid (HA-tagged) that resulted in loss of ATP7B staining in the perinuclear region of VHL-HA expressing cells (indicated with asterisks). ATP7B expression is shown in green, HA tag expression in red and nuclei were counterstained with DAPI. (**G**) Cu^S cells were stably transfected with an ATP7B overexpression plasmid. Cell viability using the Crystal Violet assay was used to detect the survival of Cu^S cells overexpressing ATP7B (+pATP7B). (**H**) Immunoblot analysis was performed to detect the protein expression of ATP7B in control Cu^S cells versus the +pATP7B Cu^S cells overexpressing ATP7B. Tubulin was used as a loading control.

Fig. III-2

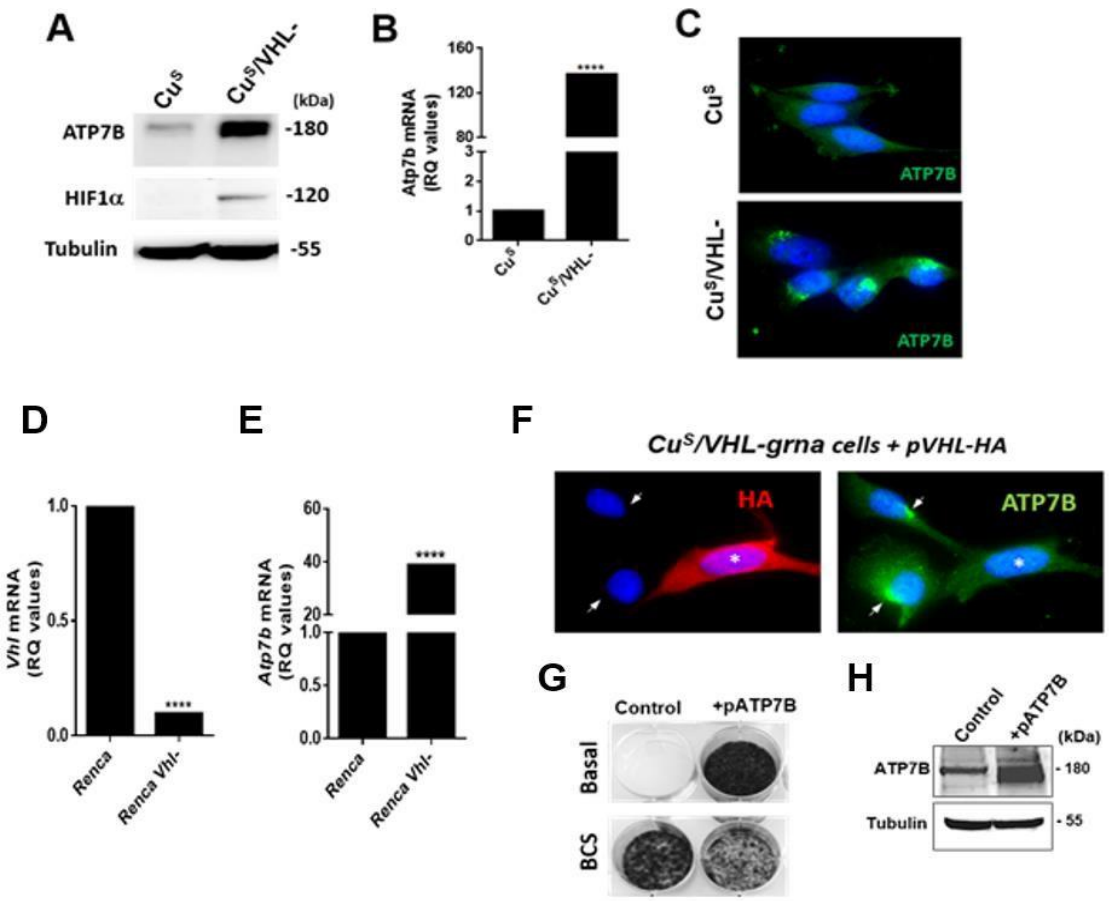
A
Cu^S
Cu^S/VHL-
(kDa)
ATP7B
-180
HIF1α
-120
Tubulin
-55
B
Atp7b mRNA (RQ values)
****
Cu^S
Cu^S/VHL-
C
Cu^S
ATP7B
Cu^S/VHL-
ATP7B
D
Vhl mRNA (RQ values)
****
Renca
Renca Vhl-
E
Atp7b mRNA (RQ values)
****
Renca
Renca Vhl-
F
Cu^S/VHL-grna cells + pVHL-HA
HA
ATP7B
G
Control
+pATP7B
Basal
BCS
H
Control
+pATP7B
(kDa)
ATP7B
- 180
Tubulin
- 55

Fig. III-3: Roxadustat induces ATP7B expression *in vitro* and *in vivo*.

(**A**) A schematic model for VHL-dependent regulation of HIF by hypoxia. Under normal levels of oxygen, HIF1α is hydroxylated by prolyl hydroxylase domain (PHD) proteins that leads to the ubiquitination of HIF1α by von Hippel-Lindau (VHL) protein to target HIF1α for proteasomal degradation. Under hypoxic conditions, HIF1α is not hydroxylated and is able to translocate to the nucleus, where it heterodimerizes with HIF1β to bind to hypoxia response elements (HREs) present in the promoter regions of target genes to regulate their expression. (**B**) Roxadustat rescues Cu^S cells in basal medium. Cu^S cells (10^3/well) were seeded in basal media containing 1% (v/v) DMSO (vehicle control), the indicated concentrations of Roxadustat or 1 μM BCS. After 5 days, cells were fixed and stained with Crystal Violet to reveal surviving colonies. (**C**) Quantitative real time PCR was performed to detect *Atp7b* mRNA levels in Cu^S cells treated with DMSO or Roxadustat (40μM). Values are expressed as the mean ± SEM (****$p < 0.0001$; $n = 3$). (**D**) Immunoblot analysis of ATP7B in Roxadustat (40μM) treated cells (for 5 days) under the conditions indicated in the figure. (**E**) Immunofluorescence detection of ATP7B in Cu^S cells exposed to Roxadustat (40μM). or DMSO. ATP7B (green) was strongly detected in perinuclear vesicles in Roxadustat-treated cells, but poorly detected in control cells. Nuclei were stained with DAPI (blue). Note that BCS (1 μM) was added to the media to permit cell survival. (**F**) Roxadustat induces hepatic expression of ATP7B in mice. Wild type C57BL/6 mice (age 8 weeks) were administered an intraperitoneal injection of Roxadustat (10 mg/kg) or DMSO (vehicle) every 24 h

over 5 days. Total membrane proteins were extracted from livers and subjected to SDS-PAGE followed by immunoblot detection of ATP7B. Ponceau staining was used as a control for protein loading. Each lane represents a different liver.

Fig. III-3

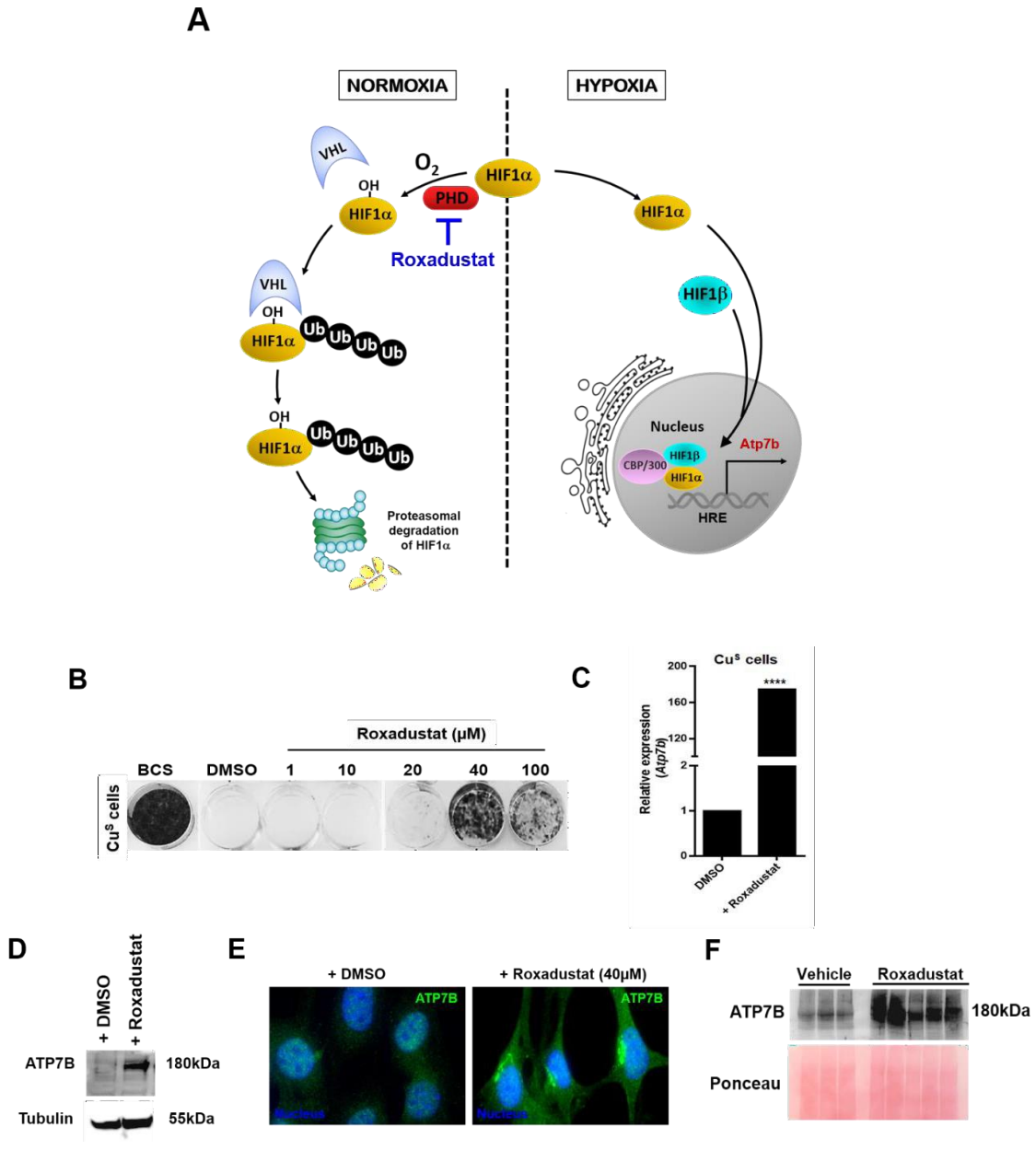
A
NORMOXIA
HYPOXIA
VHL
OH
HIF1α
O2
PHD
Roxadustat
Ub
HIF1β
Nucleus
CBP/300
Atp7b
HRE
Proteasomal degradation of HIF1α
B
Roxadustat (μM)
BCS
DMSO
1
10
20
40
100
Cu^s cells
C
Cu^s cells
Relative expression (Atp7b)
****
DMSO
+ Roxadustat
D
+ DMSO
+ Roxadustat
ATP7B
180kDa
Tubulin
55kDa
E
+ DMSO
+ Roxadustat (40μM)
ATP7B
Nucleus
F
Vehicle
Roxadustat
ATP7B
180kDa
Ponceau

Fig. III-4: Hypoxia induces ATP7B expression *in vivo*. (**A**) Cu^S cells (20 x 10^3/well) were seeded in basal media. Equal numbers of cells were seeded in media supplemented with the copper chelator, BCS, as a positive control. On Day 4, the cells were fixed and stained with Crystal Violet to reveal surviving colonies. Images were collected using light microscopy. (**B**) Quantitative real time PCR showing ATP7B expression is increased at the mRNA level in Cu^S cells under hypoxic (1% O_2) conditions (24 h). Values are expressed as the mean ± SEM (****$p < 0.0001$; $n = 3$). (**C**) Wild type C57BL/6 mice (age 8 weeks) were exposed to normoxia (21% O_2) or hypoxia (6% O_2) for 5 days. As per Fig. III-3F, ATP7B was detected in the livers of mice. Ponceau staining was used as a control for protein loading. Each lane represents a different liver.

Fig. III-4

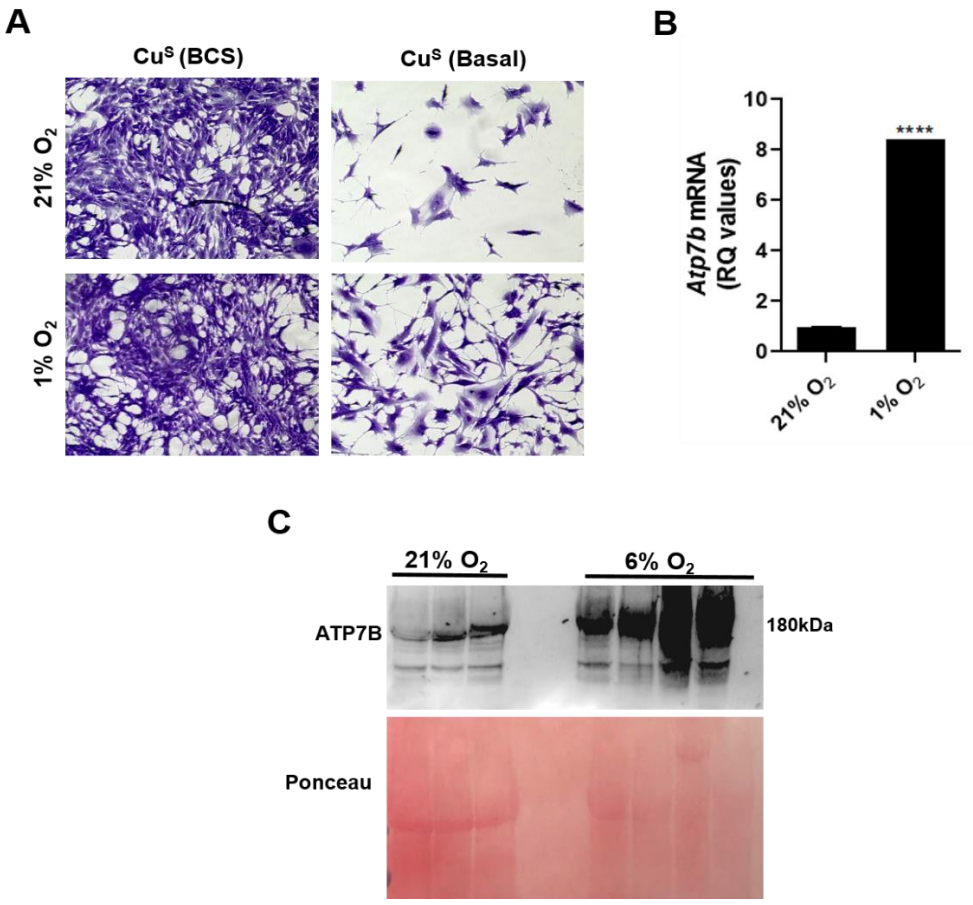
A
Cu^S (BCS)
Cu^S (Basal)
21% O2
1% O2
B
Atp7b mRNA (RQ values)
10
8
6
4
2
0
****
21% O2
1% O2
C
21% O2
6% O2
ATP7B
180kDa
Ponceau

Supplementary information

Fig. III-S1: List of gRNAs targeting *Ctr1* and *Vhl* in Cu^S cells. (**A**) Table containing list of most enriched gRNAs identified from library screen on Cu^S cells. (**B**) Table containing the list of individually tested gRNAs targeting *Ctr1* and *Vhl* in Cu^S cells.

Fig. III-S1

A

Enriched gRNAs identified from library screen

Slc31a1 gRNA 1	TAGTAAAAACACTGCCACGA
Slc31a1 gRNA 2	CAGTAAAAACACTGCCACGA
Slc31a1 gRNA 3	CTGCTGCTACTGCAATGCAT
Vhl gRNA 1	TGTATGTCCTTCCGCACACT
Vhl gRNA 2	CGCGCGTCGTGCTGCCTTTG

B

Individually tested gRNAs

Slc31a1 gRNA 1	ATGGAGATGCACCACCATATGG
Slc31a1 gRNA 2	GGACTCAAGATAGCCCGAGAGG
Vhl gRNA 1	TCTGGACTGGCTGCCTTCCG
Vhl gRNA 2	GGCGGGGGAGCCCGGTCCTG
Vhl gRNA 3	GAACTCGCGCGAGCCCTCTC

Chapter IV

Summary and future directions

4.1 Summary

Copper (Cu) is an essential micronutrient for all mammals. Although essential, Cu is also potentially toxic when it accumulates beyond cellular needs, and thus the intracellular levels of this nutrient must be precisely regulated. A delicate balance of Cu is maintained by copper-binding proteins and transporters (2). In the first part of this thesis, we investigated the relative contributions of ATP7A and metallothioneins (MTI and MTII) to copper homeostasis. To examine the importance of these proteins, we generated isogenic cell lines and it was found that cells lacking both ATP7A and metallothioneins (MTs) are extremely sensitive to copper and would only survive in media containing a copper chelator. Forced expression of these cells with either ATP7A, MTI or MTII was found to complement and rescue these copper sensitive cells in regular basal media. Performing cell viability assays, it was found that ATP7A acts as a primary mediator of copper tolerance, whereas MTs have a secondary role. The essentiality of copper-binding metallothioneins was observed in the absence of ATP7A. The lack of MTs resulted in trafficking of ATP7A from its normal steady state localization in the *trans*-Golgi complex to the plasma membrane. The discovery of this novel regulatory mechanism suggests that crosstalk exists

between ATP7A and MTs in the maintenance cellular copper homeostasis (33).

The most important aspect of the first part of this research was the discovery of an extremely copper sensitive cell line, *i.e.*, a cell line lacking ATP7A and MTI/MTII expression (referred to as the Cu^S cell line). We exploited the Cu^S cell line to isolate novel genes involved in copper metabolism. Using a CRISPR based genetic deletion screen for copper tolerance, we made the novel discovery that the von Hippel-Lindau (*Vhl*) gene regulates copper metabolism.

The latter part of the research was involved in investigating the role of the *Vhl* gene in copper metabolism. We found that disruption of the *Vhl* gene in Cu^S cells (Cu^S/VHL-), renders them resistant to copper toxicity. VHL protein is a part of the E3-ubiquitin ligase complex and is the master regulator of oxygen sensing machinery that is known to regulate the hypoxia inducible factors, HIF1α and HIF2α (133, 134). We discovered that genetic deletion of *Vhl* results in upregulation of the copper transporter, ATP7B, at both the mRNA and protein levels in Cu^s cells. Consistent with this finding, the deletion of *Vhl* was also found to upregulate *Atp7b* gene expression in a Renca cell line. Low oxygen levels and the drug Roxadustat (a prolyl hydroxylase inhibitor) facilitates the stabilization of HIF proteins, mimicking the effect of disruption of *Vhl*. Prolyl hydroxylases plays important role in the VHL/HIF pathway by hydroxylating HIF proteins at their conserved proline residues, thus enabling the VHL protein to target HIF for

subsequent degradation. Therefore, we investigated the effect of Roxadustat or hypoxia on the expression of ATP7B. We demonstrate that Roxadustat or hypoxia significantly upregulates the expression of ATP7B, both in cultured cells and hepatic tissues harvested from mice administered with Roxadustat or kept under hypoxic conditions.

Taken together, our data suggest that copper homeostasis is regulated by hypoxia *in vivo*, however, the biological purpose for this regulation remains unclear. Expression of the copper-binding protein ceruloplasmin is induced by hypoxia in a HIF-dependent manner (151) and is essential to meet the elevated iron requirements of stress erythropoiesis. Based on our findings that ATP7B expression is also induced by hypoxia, we propose that ATP7B is essential to meet the iron demands of hypoxia-induced erythropoiesis (Fig. IV-1). The oxygen carrying capacity of blood to different tissues greatly decreases during hypoxia. To meet the high demand of iron during the synthesis of new red blood cells, iron must be mobilized from hepatic stores. Hypoxia-induced upregulation of ATP7B may be required for increased copper transport to ceruloplasmin for higher hepatic iron export. Exported iron could then be utilized to produce new red blood cells in the bone marrow.

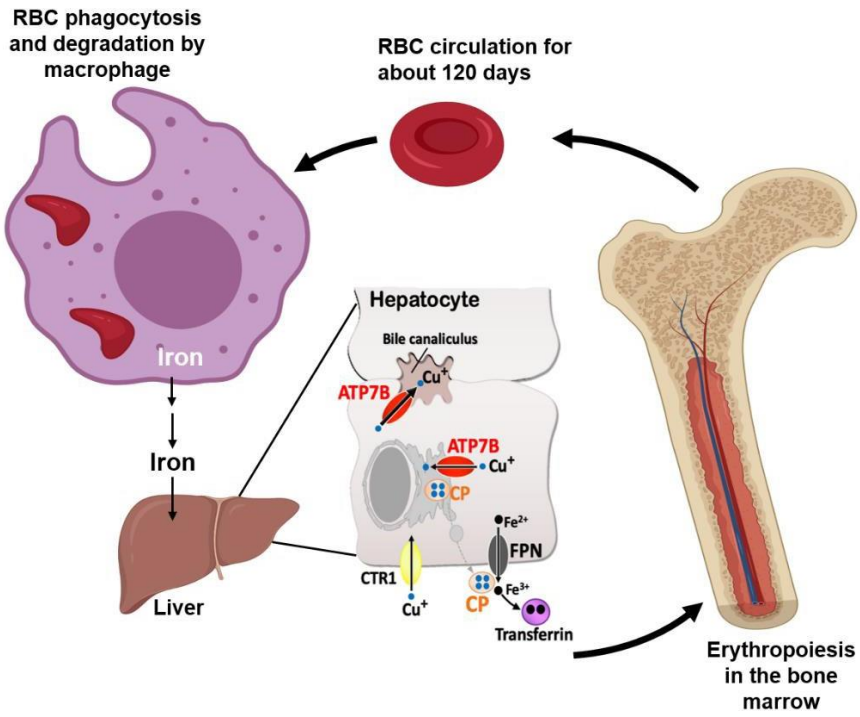

Fig. IV-1. Proposed model for the function of ATP7B in hypoxia-induced erythropoiesis. Ceruloplasmin (CP) is primarily produced in hepatocytes and acquires Cu within the *trans*-Golgi network via the ATP7B Cu transporter. ATP7B is also required for Cu excretion across the canalicular membrane into the bile. CP catalyzes the conversion of Fe^{2+} to Fe^{3+} in the plasma, which facilitates Fe^{2+} export via ferroportin (FPN) and the loading of Fe^{3+} onto transferrin. Transferrin mediates iron (Fe) delivery to the bone marrow for erythropoiesis. Red blood cells (RBCs) produced remain in circulation for about 120 days and then are degraded by macrophages. Iron (Fe^{3+}) is carried by transferrin to the liver and when required to the bone marrow for incorporation into new red blood cells.

4.2 Future work

The below mentioned approach could be used to extend the research from this project.

To investigate the mechanisms of hypoxia-induced ATP7B expression

Since our results indicate that ATP7B expression is upregulated under hypoxic conditions, as well as upon administration of the pharmacological drug Roxadustat, it will be interesting to investigate the molecular basis of ATP7B upregulation under these conditions. Based on our preliminary results, it is tempting to speculate that since HIF1 transcription factor drives the expression of a rich menu of target genes, it could also drive the expression of *Atp7b*. Since HIF proteins bind to the hypoxia response element (136) consensus sequence in target genes, we investigated if the *Atp7b* gene has the response element. We have identified two candidate HIF response elements (HREs) in the promoter regions of both mouse and human *Atp7b* genes within 1000 bp upstream of the transcription start sites. We will delete these putative HREs in the *Atp7b* promoter for expression in the luciferase reporter construct to measure the effects on promoter activity, compared to the wild type *Atp7b* promoter, under normoxic and hypoxic conditions. In addition, luciferase reporter assays will be used to evaluate whether hypoxia induces the transcription of ATP7B. Renilla luciferase fusion constructs containing upstream promoter regions of the mouse and human *Atp7b* genes will be transiently transfected into HEK293 cells

together with a luciferase co-reporter plasmid to control for transfection efficiency. Cells will be incubated for 24 h under normoxia or hypoxia (1% O_2) and promoter activity will be measured as a function of Renilla/Firefly luciferase activities. Finally, we will perform chromatin immunoprecipitation (ChIP) experiments to directly measure HIF binding to the promoter region of ATP7B in cell lines and in the livers of mice exposed to normoxia and hypoxia, as described (152).

Furthermore, we will investigate whether hypoxia-induced expression of ATP7B is absent in cells devoid of HIF signaling. For this purpose, we have obtained a hepatoma cell line lacking HIF1β from ATCC (#CRL-2717), as well as control cells that express HIF1β (ATCC# CRL-2712). HIF1β is essential for HIF signaling as an obligatory heterodimeric partner with HIF1α and HIF2α (Fig. III-3A) (153). Thus, these HIF1β+ and HIF1β- cell lines will be incubated under normoxic or hypoxic (1% O_2) conditions and ATP7B expression (mRNA and protein) will be evaluated.

To complement these studies, we will also evaluate both Cu tolerance and ATP7B expression in Cu^S cells that have been stably transfected with plasmids encoding HIF1α and HIF2α mutants that are resistant to oxygen-mediated degradation (Addgene plasmids #19005 and 19006).

To test the therapeutic potential of hypoxia or Roxadustat in a mouse model of Wilson disease

ATP7B and Wilson disease: ATP7B is expressed primarily in hepatocytes, where it excretes Cu from the body via the bile. Consequently, the loss of ATP7B function in Wilson patients results in copper accumulation in the liver, which if untreated results in liver failure and mortality. Neurological symptoms can also present in certain patients including tremor, dysphagia and dysarthria which is associated with accumulation of copper in the brain. The Cu-chelating drug, penicillamine, is the first line of therapy for Wilson disease patients, however, 30% cannot tolerate this treatment due to numerous side effects (154). Zinc salts can be used to reduce the absorption of dietary copper, but this is typically reserved for pre-symptomatic patients, as it is generally not considered to be effective in patients with hepatic disease. Medical therapy is rarely effective in patients presenting with acute liver failure due to the time required to remove toxic copper from the organ. Liver transplantation is often necessary in patients with acute liver failure (85). Current therapies for Wilson disease patients are poorly tolerated in a significant proportion of patients and can worsen neurological symptoms. Thus, there is a need to develop safe and efficacious treatment options for Wilson disease patients.

Repurposing the prolyl hydroxylase inhibitor, Roxadustat: Roxadustat is used as a treatment for anemia in patients with kidney disease (155). Our discovery that this drug induces the expression of ATP7B *in vivo* raises the

exciting possibility that Roxadustat could be repurposed to treat diseases caused by mutations in ATP7B. Mutations in the ATP7B result in Wilson disease, a disorder of copper overload in the liver and brain. For example, one of the most common ATP7B mutations, H1069Q, is known to reduce the abundance of ATP7B protein, but does not eliminate its copper transport activity (156). We hypothesize that Roxadustat (or hypoxia) could be an effective treatment in patients with the H1069Q variant or similar hypomorphic mutations in ATP7B protein. We will test this hypothesis by investigating the therapeutic efficacy of Roxadustat on hepatic Cu accumulation and liver pathology in mice harboring the ATP7B-H1071Q (Applied stem cell: ASKI-18001) mutation which is equivalent to the human H1069Q mutation. We hypothesize that Roxadustat-induced ATP7B expression will ameliorate the hyperaccumulation of Cu and reduce pathology in a mouse model of Wilson disease, which should help translate this therapy to human patients.

References

1. Yoshii J, Yoshiji H, Kuriyama S, Ikenaka Y, Noguchi R, Okuda H, et al. The copper-chelating agent, trientine, suppresses tumor development and angiogenesis in the murine hepatocellular carcinoma cells. Int J Cancer. 2001;94(6):768-73.

2. Nevitt T, Ohrvik H, Thiele DJ. Charting the travels of copper in eukaryotes from yeast to mammals. Biochim Biophys Acta. 2012;1823(9):1580-93.

3. Ochiai EI. Copper and the biological evolution. Biosystems. 1983;16(2):81-6.

4. Chi Fru E, Rodriguez NP, Partin CA, Lalonde SV, Andersson P, Weiss DJ, et al. Cu isotopes in marine black shales record the Great Oxidation Event. Proc Natl Acad Sci U S A. 2016;113(18):4941-6.

5. Macomber L, Imlay JA. The iron-sulfur clusters of dehydratases are primary intracellular targets of copper toxicity. Proc Natl Acad Sci U S A. 2009;106(20):8344-9.

6. Pierson H, Yang H, Lutsenko S. Copper transport and disease: what can we Learn from organoids? Annu Rev Nutr. 2019;39:75-94.

7. Turnlund JR, Keyes WR, Anderson HL, Acord LL. Copper absorption and retention in young men at three levels of dietary copper by use of the stable isotope 65Cu. Am J Clin Nutr. 1989;49(5):870-8.

8. Prohaska JR. Impact of copper deficiency in humans. Ann N Y Acad Sci. 2014;1314:1-5.

9. Zhou B, Gitschier J. hCTR1: a human gene for copper uptake identified by complementation in yeast. Proc Natl Acad Sci U S A. 1997;94(14):7481-6.

10. Kuo YM, Zhou B, Cosco D, Gitschier J. The copper transporter CTR1 provides an essential function in mammalian embryonic development. Proc Natl Acad Sci U S A. 2001;98(12):6836-41.

11. Lee J, Pena MM, Nose Y, Thiele DJ. Biochemical characterization of the human copper transporter Ctr1. J Biol Chem. 2002;277(6):4380-7.

12. Aller SG, Unger VM. Projection structure of the human copper transporter CTR1 at 6-A resolution reveals a compact trimer with a novel channel-like architecture. Proc Natl Acad Sci U S A. 2006;103(10):3627-32.

13. Ren F, Logeman BL, Zhang X, Liu Y, Thiele DJ, Yuan P. X-ray structures of the high-affinity copper transporter Ctr1. Nat Commun. 2019;10(1):1386.

14. Puig S, Lee J, Lau M, Thiele DJ. Biochemical and genetic analyses of yeast and human high affinity copper transporters suggest a conserved mechanism for copper uptake. J Biol Chem. 2002;277(29):26021-30.

15. Drakesmith H, Nemeth E, Ganz T. Ironing out Ferroportin. Cell Metab. 2015;22(5):777-87.

16. Ramos D, Mar D, Ishida M, Vargas R, Gaite M, Montgomery A, et al. Mechanism of copper uptake from blood plasma ceruloplasmin by mammalian cells. PLoS One. 2016;11(3):e0149516.

17. Meyer LA, Durley AP, Prohaska JR, Harris ZL. Copper transport and metabolism are normal in aceruloplasminemic mice. J Biol Chem. 2001;276(39):36857-61.

18. Linder MC. Ceruloplasmin and other copper binding components of blood plasma and their functions: an update. Metallomics. 2016;8(9):887-905.

19. Gray LW, Peng F, Molloy SA, Pendyala VS, Muchenditsi A, Muzik O, et al. Urinary copper elevation in a mouse model of Wilson's disease is a regulated process to specifically decrease the hepatic copper load. PLoS One. 2012;7(6):e38327.

20. Lin C, Zhang Z, Wang T, Chen C, James Kang Y. Copper uptake by DMT1: a compensatory mechanism for CTR1 deficiency in human umbilical vein endothelial cells. Metallomics. 2015;7(8):1285-9.

21. Shawki A, Anthony SR, Nose Y, Engevik MA, Niespodzany EJ, Barrientos T, et al. Intestinal DMT1 is critical for iron absorption in the mouse but is not required for the absorption of copper or manganese. Am J Physiol Gastrointest Liver Physiol. 2015;309(8):G635-47.

22. Nose Y, Kim BE, Thiele DJ. Ctr1 drives intestinal copper absorption and is essential for growth, iron metabolism, and neonatal cardiac function. Cell Metab. 2006;4(3):235-44.

23. Hassett R, Kosman DJ. Evidence for Cu(II) reduction as a component of copper uptake by Saccharomyces cerevisiae. J Biol Chem. 1995;270(1):128-34.

24. Ohgami RS, Campagna DR, McDonald A, Fleming MD. The Steap proteins are metalloreductases. Blood. 2006;108(4):1388-94.

25. Song IS, Chen HH, Aiba I, Hossain A, Liang ZD, Klomp LW, et al. Transcription factor Sp1 plays an important role in the regulation of copper homeostasis in mammalian cells. Mol Pharmacol. 2008;74(3):705-13.

26. Liang ZD, Tsai WB, Lee MY, Savaraj N, Kuo MT. Specificity protein 1 (sp1) oscillation is involved in copper homeostasis maintenance by regulating human high-affinity copper transporter 1 expression. Mol Pharmacol. 2012;81(3):455-64.

27. Petris MJ, Smith K, Lee J, Thiele DJ. Copper-stimulated endocytosis and degradation of the human copper transporter, hCtr1. J Biol Chem. 2003;278(11):9639-46.

28. Maryon EB, Molloy SA, Ivy K, Yu H, Kaplan JH. Rate and regulation of copper transport by human copper transporter 1 (hCTR1). J Biol Chem. 2013;288(25):18035-46.

29. Ohrvik H, Logeman B, Turk B, Reinheckel T, Thiele DJ. Cathepsin protease controls copper and cisplatin accumulation via cleavage of the Ctr1 metal-binding ectodomain. J Biol

Chem. 2016;291(27):13905-16.

30. Ohrvik H, Nose Y, Wood LK, Kim BE, Gleber SC, Ralle M, et al. Ctr2 regulates biogenesis of a cleaved form of mammalian Ctr1 metal transporter lacking the copper- and cisplatin-binding ecto-domain. Proc Natl Acad Sci U S A. 2013;110(46):E4279-88.

31. Logeman BL, Wood LK, Lee J, Thiele DJ. Gene duplication and neo-functionalization in the evolutionary and functional divergence of the metazoan copper transporters Ctr1 and Ctr2. J Biol Chem. 2017;292(27):11531-46.

32. Culotta V, Scott RA. Metals in cells: Wiley; 2016.

33. Gudekar N, Shanbhag V, Wang Y, Ralle M, Weisman GA, Petris MJ. Metallothioneins regulate ATP7A trafficking and control cell viability during copper deficiency and excess. Sci Rep. 2020;10(1):7856.

34. Jiang X, Chen J, Bajic A, Zhang C, Song X, Carroll SL, et al. Quantitative real-time imaging of glutathione. Nat Commun. 2017;8:16087.

35. Maryon EB, Molloy SA, Kaplan JH. Cellular glutathione plays a key role in copper uptake mediated by human copper transporter 1. Am J Physiol Cell Physiol. 2013;304(8):C768-79.

36. Meister A, Anderson ME. Glutathione. Annu Rev Biochem. 1983;52:711-60.

37. DeLeve LD, Kaplowitz N. Importance and regulation of hepatic glutathione. Semin Liver Dis. 1990;10(4):251-66.

38. Suthanthiran M, Anderson ME, Sharma VK, Meister A. Glutathione regulates activation-dependent DNA synthesis in highly purified normal human T lymphocytes stimulated via the CD2 and CD3 antigens. Proc Natl Acad Sci U S A. 1990;87(9):3343-7.

39. Forman HJ, Zhang H, Rinna A. Glutathione: overview of its protective roles, measurement, and biosynthesis. Mol Aspects Med. 2009;30(1-2):1-12.

40. Timon-Gomez A, Nyvltova E, Abriata LA, Vila AJ, Hosler J, Barrientos A. Mitochondrial cytochrome c oxidase biogenesis: Recent developments. Semin Cell Dev Biol. 2018;76:163-78.

41. Cobine PA, Ojeda LD, Rigby KM, Winge DR. Yeast contain a non-proteinaceous pool of copper in the mitochondrial matrix. J Biol Chem. 2004;279(14):14447-55.

42. Vest KE, Leary SC, Winge DR, Cobine PA. Copper import into the mitochondrial matrix in Saccharomyces cerevisiae is mediated by Pic2, a mitochondrial carrier family protein. J Biol Chem. 2013;288(33):23884-92.

43. Vest KE, Wang J, Gammon MG, Maynard MK, White OL, Cobine JA, et al. Overlap of copper and iron uptake systems in mitochondria in Saccharomyces cerevisiae. Open Biol. 2016;6(1):150223.

44. Boulet A, Vest KE, Maynard MK, Gammon MG, Russell AC, Mathews AT, et al. The mammalian phosphate carrier SLC25A3 is a mitochondrial copper transporter required for cytochrome c oxidase biogenesis. J Biol Chem. 2018;293(6):1887-96.

45. Winge DR. Filling the mitochondrial copper pool. J Biol Chem. 2018;293(6):1897-8.

46. Polishchuk R, Lutsenko S. Golgi in copper homeostasis: a view from the membrane trafficking field. Histochem Cell Biol. 2013;140(3):285-95.

47. Petris MJ, Mercer JF, Culvenor JG, Lockhart P, Gleeson PA, Camakaris J. Ligand-regulated transport of the Menkes copper P-type ATPase efflux pump from the Golgi apparatus to the plasma membrane: a novel mechanism of regulated trafficking. EMBO J. 1996;15(22):6084-95.

48. Hung IH, Suzuki M, Yamaguchi Y, Yuan DS, Klausner RD, Gitlin JD. Biochemical characterization of the Wilson disease protein and functional expression in the yeast Saccharomyces cerevisiae. J Biol Chem. 1997;272(34):21461-6.

49. Barry AN, Shinde U, Lutsenko S. Structural organization of human Cu-transporting ATPases: learning from building blocks. J Biol Inorg Chem. 2010;15(1):47-59.

50. Dyla M, Kjaergaard M, Poulsen H, Nissen P. Structure and mechanism of P-Type ATPase ion pumps. Annu Rev Biochem. 2020;89:583-603.

51. Gourdon P, Liu XY, Skjorringe T, Morth JP, Moller LB, Pedersen BP, et al. Crystal structure of a copper-transporting PIB-type ATPase. Nature. 2011;475(7354):59-64.

52. Pase L, Voskoboinik I, Greenough M, Camakaris J. Copper stimulates trafficking of a distinct pool of the Menkes copper ATPase (ATP7A) to the plasma membrane and diverts it into a rapid recycling pool. Biochem J. 2004;378(Pt 3):1031-7.

53. Hartwig C, Zlatic SA, Wallin M, Vrailas-Mortimer A, Fahrni CJ, Faundez V. Trafficking mechanisms of P-type ATPase copper transporters. Curr Opin Cell Biol. 2019;59:24-33.

54. Monty JF, Llanos RM, Mercer JF, Kramer DR. Copper exposure induces trafficking of the menkes protein in intestinal epithelium of ATP7A transgenic mice. J Nutr. 2005;135(12):2762-6.

55. Roelofsen H, Wolters H, Van Luyn MJ, Miura N, Kuipers F, Vonk RJ. Copper-induced apical trafficking of ATP7B in polarized hepatoma cells provides a mechanism for biliary copper excretion. Gastroenterology. 2000;119(3):782-93.

56. Polishchuk EV, Concilli M, Iacobacci S, Chesi G, Pastore N, Piccolo P, et al. Wilson disease protein ATP7B utilizes lysosomal exocytosis to maintain copper homeostasis. Dev Cell. 2014;29(6):686-700.

57. Zhu S, Shanbhag V, Hodgkinson VL, Petris MJ. Multiple di-leucines in the ATP7A copper transporter are required for retrograde trafficking to the trans-Golgi network. Metallomics. 2016;8(9):993-1001.

58. Francis MJ, Jones EE, Levy ER, Martin RL, Ponnambalam S, Monaco AP. Identification of a di-leucine motif within the C terminus domain of the Menkes disease protein that mediates endocytosis from the plasma membrane. J Cell Sci. 1999;112 (Pt 11):1721-32.

59. Holloway ZG, Velayos-Baeza A, Howell GJ, Levecque C, Ponnambalam S, Sztul E, et al. Trafficking of the Menkes copper transporter ATP7A is regulated by clathrin-, AP-2-, AP-1-, and Rab22-dependent steps. Mol Biol Cell. 2013;24(11):1735-48, S1-8.

60. Francis MJ, Jones EE, Levy ER, Ponnambalam S, Chelly J, Monaco AP. A Golgi localization signal identified in the Menkes recombinant protein. Hum Mol Genet. 1998;7(8):1245-52.

61. Greenough M, Pase L, Voskoboinik I, Petris MJ, O'Brien AW, Camakaris J. Signals regulating trafficking of Menkes (MNK; ATP7A) copper-translocating P-type ATPase in polarized MDCK cells. Am J Physiol Cell Physiol. 2004;287(5):C1463-71.

62. Braiterman L, Nyasae L, Guo Y, Bustos R, Lutsenko S, Hubbard A. Apical targeting and Golgi retention signals reside within a 9-amino acid sequence in the copper-ATPase, ATP7B. Am J Physiol Gastrointest Liver Physiol. 2009;296(2):G433-44.

63. Strausak D, La Fontaine S, Hill J, Firth SD, Lockhart PJ, Mercer JF. The role of GMXCXXC metal binding sites in the copper-induced redistribution of the Menkes protein. J Biol Chem. 1999;274(16):11170-7.

64. Goodyer ID, Jones EE, Monaco AP, Francis MJ. Characterization of the Menkes protein copper-binding domains and their role in copper-induced protein relocalization. Hum Mol Genet. 1999;8(8):1473-8.

65. Petris MJ, Voskoboinik I, Cater M, Smith K, Kim BE, Llanos RM, et al. Copper-regulated trafficking of the Menkes disease copper ATPase is associated with formation of a phosphorylated catalytic intermediate. J Biol Chem. 2002;277(48):46736-42.

66. Cater MA, La Fontaine S, Mercer JF. Copper binding to the N-terminal metal-binding sites or the CPC motif is not essential for copper-induced trafficking of the human Wilson protein (ATP7B). Biochem J. 2007;401(1):143-53.

67. Skjorringe T, Amstrup Pedersen P, Salling Thorborg S, Nissen P, Gourdon P, Birk Moller L.

Characterization of ATP7A missense mutants suggests a correlation between intracellular trafficking and severity of Menkes disease. Sci Rep. 2017;7(1):757.

68. Kim BE, Smith K, Petris MJ. A copper treatable Menkes disease mutation associated with defective trafficking of a functional Menkes copper ATPase. J Med Genet. 2003;40(4):290-5.

69. Valnot I, Osmond S, Gigarel N, Mehaye B, Amiel J, Cormier-Daire V, et al. Mutations of the SCO1 gene in mitochondrial cytochrome c oxidase deficiency with neonatal-onset hepatic failure and encephalopathy. Am J Hum Genet. 2000;67(5):1104-9.

70. Papadopoulou LC, Sue CM, Davidson MM, Tanji K, Nishino I, Sadlock JE, et al. Fatal infantile cardioencephalomyopathy with COX deficiency and mutations in SCO2, a COX assembly gene. Nat Genet. 1999;23(3):333-7.

71. Ghosh A, Trivedi PP, Timbalia SA, Griffin AT, Rahn JJ, Chan SS, et al. Copper supplementation restores cytochrome c oxidase assembly defect in a mitochondrial disease model of COA6 deficiency. Hum Mol Genet. 2014;23(13):3596-606.

72. Szklarczyk R, Wanschers BF, Nijtmans LG, Rodenburg RJ, Zschocke J, Dikow N, et al. A mutation in the FAM36A gene, the human ortholog of COX20, impairs cytochrome c oxidase assembly and is associated with ataxia and muscle hypotonia. Hum Mol Genet. 2013;22(4):656-67.

73. Kaler SG. ATP7A-related copper transport diseases-emerging concepts and future trends. Nature Rev Neurol. 2011;7(1):15-29.

74. Wang Y, Zhu S, Hodgkinson V, Prohaska JR, Weisman GA, Gitlin JD, et al. Maternofetal and neonatal copper requirements revealed by enterocyte-specific deletion of the Menkes disease protein. Am J Physiol Gastrointest Liver Physiol. 2012;303(11):G1236-44.

75. Telianidis J, Hung YH, Materia S, Fontaine SL. Role of the P-Type ATPases, ATP7A and ATP7B in brain copper homeostasis. Front Aging Neurosci. 2013;5:44.

76. Kaler SG. Translational research investigations on ATP7A: an important human copper ATPase. Ann N Y Acad Sci. 2014;1314:64-8.

77. Haddad MR, Choi EY, Zerfas PM, Yi L, Martinelli D, Sullivan P, et al. Cerebrospinal fluid-directed rAAV9-rsATP7A plus subcutaneous copper histidinate advance survival and outcomes in a Menkes disease mouse model. Mol Ther Methods Clin Dev. 2018;10:165-78.

78. Guthrie LM, Soma S, Yuan S, Silva A, Zulkifli M, Snavely TC, et al. Elesclomol alleviates Menkes pathology and mortality by escorting Cu to cuproenzymes in mice. Science. 2020;368(6491):620-5.

79. Hedley D, Shamas-Din A, Chow S, Sanfelice D, Schuh AC, Brandwein JM, et al. A phase I study of elesclomol sodium in patients with acute myeloid leukemia. Leuk Lymphoma. 2016;57(10):2437-40.

80. Kaler SG, Gallo LK, Proud VK, Percy AK, Mark Y, Segal NA, et al. Occipital horn syndrome and a mild Menkes phenotype associated with splice site mutations at the MNK locus. Nat Genet. 1994;8(2):195-202.

81. Kennerson ML, Nicholson GA, Kaler SG, Kowalski B, Mercer JF, Tang J, et al. Missense mutations in the copper transporter gene ATP7A cause X-linked distal hereditary motor neuropathy. Am J Hum Genet. 2010;86(3):343-52.

82. Hodgkinson VL, Dale JM, Garcia ML, Weisman GA, Lee J, Gitlin JD, et al. X-linked spinal muscular atrophy in mice caused by autonomous loss of ATP7A in the motor neuron. J Pathol. 2015;236(2):241-50.

83. Yi L, Donsante A, Kennerson ML, Mercer JF, Garbern JY, Kaler SG. Altered intracellular localization and valosin-containing protein (p97 VCP) interaction underlie ATP7A-related distal motor neuropathy. Hum Mol Genet. 2012;21(8):1794-807.

84. Czlonkowska A, Litwin T, Dusek P, Ferenci P, Lutsenko S, Medici V, et al. Wilson disease.

Nat Rev Dis Primers. 2018;4(1):21.

85. Saroli Palumbo C, Schilsky ML. Clinical practice guidelines in Wilson disease. Ann Transl Med. 2019;7(Suppl 2):S65.

86. Martinelli D, Travaglini L, Drouin CA, Ceballos-Picot I, Rizza T, Bertini E, et al. MEDNIK syndrome: a novel defect of copper metabolism treatable by zinc acetate therapy. Brain. 2013;136(Pt 3):872-81.

87. Setty SR, Tenza D, Sviderskaya EV, Bennett DC, Raposo G, Marks MS. Cell-specific ATP7A transport sustains copper-dependent tyrosinase activity in melanosomes. Nature. 2008;454(7208):1142-6.

88. Burkhead JL, Reynolds KA, Abdel-Ghany SE, Cohu CM, Pilon M. Copper homeostasis. New Phytol. 2009;182(4):799-816.

89. Arioz C, Wittung-Stafshede P. Folding of copper proteins: role of the metal? Q Rev Biophys. 2018;51:e4.

90. Smith AD, Logeman BL, Thiele DJ. Copper acquisition and utilization in fungi. Annu Rev Microbiol. 2017;71:597-623.

91. Banci L, Bertini I, Ciofi-Baffoni S, Kozyreva T, Zovo K, Palumaa P. Affinity gradients drive copper to cellular destinations. Nature. 2010;465(7298):645-8.

92. Dolgova NV, Yu C, Cvitkovic JP, Hodak M, Nienaber KH, Summers KL, et al. Binding of copper and cisplatin to Atox1 is mediated by glutathione through the formation of metal-sulfur clusters. Biochem. 2017;56(24):3129-41.

93. Robinson NJ, Winge DR. Copper metallochaperones. Annu Rev Biochem. 2010;79:537-62.

94. Magistrato A, Pavlin M, Qasem Z, Ruthstein S. Copper trafficking in eukaryotic systems: current knowledge from experimental and computational efforts. Curr Opin Struct Biol. 2019;58:26-33.

95. Ladomersky E, Petris MJ. Copper tolerance and virulence in bacteria. Metallomics. 2015;7(6):957-64.

96. Camakaris J, Petris MJ, Bailey L, Shen P, Lockhart P, Glover TW, et al. Gene amplification of the Menkes (MNK; ATP7A) P-type ATPase gene of CHO cells is associated with copper resistance and enhanced copper efflux. Hum Mol Genet. 1995;4(11):2117-23.

97. Yamaguchi Y, Heiny ME, Suzuki M, Gitlin JD. Biochemical characterization and intracellular localization of the Menkes disease protein. Proc Natl Acad Sci U S A. 1996;93(24):14030-5.

98. Petris MJ, Strausak D, Mercer JF. The Menkes copper transporter is required for the activation of tyrosinase. Hum Mol Genet. 2000;9(19):2845-51.

99. Calvo J, Jung H, Meloni G. Copper metallothioneins. IUBMB Life. 2017;69(4):236-45.

100. Karin M, Najarian R, Haslinger A, Valenzuela P, Welch J, Fogel S. Primary structure and transcription of an amplified genetic locus: the CUP1 locus of yeast. Proc Natl Acad Sci U S A. 1984;81(2):337-41.

101. Thirumoorthy N, Manisenthil Kumar KT, Shyam Sundar A, Panayappan L, Chatterjee M. Metallothionein: an overview. World J Gastroenterol. 2007;13(7):993-6.

102. Uchida Y, Takio K, Titani K, Ihara Y, Tomonaga M. The growth inhibitory factor that is deficient in the Alzheimer's disease brain is a 68 amino acid metallothionein-like protein. Neuron. 1991;7(2):337-47.

103. Quaife CJ, Findley SD, Erickson JC, Froelick GJ, Kelly EJ, Zambrowicz BP, et al. Induction of a new metallothionein isoform (MT-IV) occurs during differentiation of stratified squamous

epithelia. Biochem. 1994;33(23):7250-9.

104. Gunther V, Lindert U, Schaffner W. The taste of heavy metals: gene regulation by MTF-1. Biochim Biophys Acta. 2012;1823(9):1416-25.

105. Shaw CF, 3rd, Savas MM, Petering DH. Ligand substitution and sulfhydryl reactivity of metallothionein. Methods Enzymol. 1991;205:401-14.

106. Tapia L, Gonzalez-Aguero M, Cisternas MF, Suazo M, Cambiazo V, Uauy R, et al. Metallothionein is crucial for safe intracellular copper storage and cell survival at normal and supra-physiological exposure levels. Biochem J. 2004;378(Pt 2):617-24.

107. Palmiter RD. Constitutive expression of metallothionein-III (MT-III), but not MT-I, inhibits growth when cells become zinc deficient. Toxicol Appl Pharmacol. 1995;135(1):139-46.

108. Park JD, Liu Y, Klaassen CD. Protective effect of metallothionein against the toxicity of cadmium and other metals(1). Toxicology. 2001;163(2-3):93-100.

109. Kelly EJ, Palmiter RD. A murine model of Menkes disease reveals a physiological function of metallothionein. Nat Genet. 1996;13(2):219-22.

110. Wang Y, Zhu S, Weisman GA, Gitlin JD, Petris MJ. Conditional knockout of the Menkes disease copper transporter demonstrates its critical role in embryogenesis. PLoS One. 2012;7(8):e43039.

111. Masters BA, Kelly EJ, Quaife CJ, Brinster RL, Palmiter RD. Targeted disruption of metallothionein I and II genes increases sensitivity to cadmium. Proc Natl Acad Sci U S A. 1994;91(2):584-8.

112. Ostergaard H, Tachibana C, Winther JR. Monitoring disulfide bond formation in the eukaryotic cytosol. J Cell Biol. 2004;166(3):337-45.

113. Freedman JH, Ciriolo MR, Peisach J. The role of glutathione in copper metabolism and toxicity. J Biol Chem. 1989;264(10):5598-605.

114. Semprine J, Ferrarotti N, Musacco-Sebio R, Saporito-Magrina C, Fuda J, Torti H, et al. Brain antioxidant responses to acute iron and copper intoxications in rats. Metallomics. 2014;6(11):2083-9.

115. La Fontaine SL, Firth SD, Camakaris J, Englezou A, Theophilos MB, Petris MJ, et al. Correction of the copper transport defect of Menkes patient fibroblasts by expression of the Menkes and Wilson ATPases. J Biol Chem. 1998;273(47):31375-80.

116. Gupta A, Bhattacharjee A, Dmitriev OY, Nokhrin S, Braiterman L, Hubbard AL, et al. Cellular copper levels determine the phenotype of the Arg875 variant of ATP7B/Wilson disease protein. Proc Natl Acad Sci U S A. 2011;108(13):5390-5.

117. Shanbhag V, Jasmer-McDonald K, Zhu S, Martin AL, Gudekar N, Khan A, et al. ATP7A delivers copper to the lysyl oxidase family of enzymes and promotes tumorigenesis and metastasis. Proc Natl Acad Sci U S A. 2019;116(14):6836-41.

118. Palmiter RD. Regulation of metallothionein genes by heavy metals appears to be mediated by a zinc-sensitive inhibitor that interacts with a constitutively active transcription factor, MTF-1. Proc Natl Acad Sci U S A. 1994;91(4):1219-23.

119. Vallieres C, Holland SL, Avery SV. Mitochondrial ferredoxin determines vulnerability of cells to copper excess. Cell Chem Biol. 2017;24(10):1228-37 e3.

120. Bhattacharjee A, Yang H, Duffy M, Robinson E, Conrad-Antoville A, Lu YW, et al. The activity of Menkes disease protein ATP7A is essential for redox balance in mitochondria. J Biol Chem. 2016;291(32):16644-58.

121. Carroll MC, Girouard JB, Ulloa JL, Subramaniam JR, Wong PC, Valentine JS, et al. Mechanisms for activating Cu- and Zn-containing superoxide dismutase in the absence of the CCS Cu chaperone. Proc Natl Acad Sci U S A. 2004;101(16):5964-9.

122. Hamza I, Prohaska J, Gitlin JD. Essential role for Atox1 in the copper-mediated

intracellular trafficking of the Menkes ATPase. Proc Natl Acad Sci U S A. 2003;100(3):1215-20.

123. MacDiarmid CW, Milanick MA, Eide DJ. Induction of the ZRC1 metal tolerance gene in zinc-limited yeast confers resistance to zinc shock. J Biol Chem. 2003;278(17):15065-72.

124. Kumar N, Gross JB, Jr., Ahlskog JE. Copper deficiency myelopathy produces a clinical picture like subacute combined degeneration. Neurology. 2004;63(1):33-9.

125. Jaiser SR, Winston GP. Copper deficiency myelopathy. J Neurol. 2010;257(6):869-81.

126. Afrin LB. Fatal copper deficiency from excessive use of zinc-based denture adhesive. Am J Med Sci. 2010;340(2):164-8.

127. Miyake M, Goodison S, Lawton A, Gomes-Giacoia E, Rosser CJ. Angiogenin promotes tumoral growth and angiogenesis by regulating matrix metallopeptidase-2 expression via the ERK1/2 pathway. Oncogene. 2015;34(7):890-901.

128. Southern PJ, Berg P. Transformation of mammalian cells to antibiotic resistance with a bacterial gene under control of the SV40 early region promoter. J Mol Appl Genet. 1982;1(4):327-41.

129. Feoktistova M, Geserick P, Leverkus M. Crystal Violet assay for determining viability of cultured cells. Cold Spring Harb Protoc. 2016;2016(4):pdb prot087379.

130. Zhu S, Shanbhag V, Wang Y, Lee J, Petris M. A role for the ATP7A copper transporter in tumorigenesis and cisplatin resistance. J Cancer. 2017;8(11):1952-8.

131. Mao X, Kim BE, Wang F, Eide DJ, Petris MJ. A histidine-rich cluster mediates the ubiquitination and degradation of the human zinc transporter, hZIP4, and protects against zinc cytotoxicity. J Biol Chem. 2007;282(10):6992-7000.

132. Rosencrantz R, Schilsky M. Wilson disease: pathogenesis and clinical considerations in diagnosis and treatment. Semin Liver Dis. 2011;31(3):245-59.

133. Iwai K, Yamanaka K, Kamura T, Minato N, Conaway RC, Conaway JW, et al. Identification of the von Hippel-lindau tumor-suppressor protein as part of an active E3 ubiquitin ligase complex. Proc Natl Acad Sci U S A. 1999;96(22):12436-41.

134. Semenza GL. HIF-1 and human disease: one highly involved factor. Genes Dev. 2000;14(16):1983-91.

135. Ivan M, Kondo K, Yang H, Kim W, Valiando J, Ohh M, et al. HIFalpha targeted for VHL-mediated destruction by proline hydroxylation: implications for O2 sensing. Science. 2001;292(5516):464-8.

136. Schietke R, Warnecke C, Wacker I, Schodel J, Mole DR, Campean V, et al. The lysyl oxidases LOX and LOXL2 are necessary and sufficient to repress E-cadherin in hypoxia: insights into cellular transformation processes mediated by HIF-1. J Biol Chem. 2010;285(9):6658-69.

137. Chen PS, Chiu WT, Hsu PL, Lin SC, Peng IC, Wang CY, et al. Pathophysiological implications of hypoxia in human diseases. J Biomed Sci. 2020;27(1):63.

138. Ganz T, Nemeth E. Iron metabolism: interactions with normal and disordered erythropoiesis. Cold Spring Harb Perspect Med. 2012;2(5):a011668.

139. Nicolas G, Chauvet C, Viatte L, Danan JL, Bigard X, Devaux I, et al. The gene encoding the iron regulatory peptide hepcidin is regulated by anemia, hypoxia, and inflammation. J Clin Invest. 2002;110(7):1037-44.

140. Finch C. Regulators of iron balance in humans. Blood. 1994;84(6):1697-702.

141. Musci G, Polticelli F, Bonaccorsi di Patti MC. Ceruloplasmin-ferroportin system of iron traffic in vertebrates. World J Biol Chem. 2014;5(2):204-15.

142. Prohaska JR, Gybina AA. Intracellular copper transport in mammals. J Nutr. 2004;134(5):1003-6.

143. Haase VH. The VHL tumor suppressor: master regulator of HIF. Curr Pharm Des.

2009;15(33):3895-903.

144. Bruick RK, McKnight SL. A conserved family of prolyl-4-hydroxylases that modify HIF. Science. 2001;294(5545):1337-40.

145. Arsenault PR, Heaton-Johnson KJ, Li LS, Song D, Ferreira VS, Patel N, et al. Identification of prolyl hydroxylation modifications in mammalian cell proteins. Proteomics. 2015;15(7):1259-67.

146. Strowitzki MJ, Cummins EP, Taylor CT. Protein Hydroxylation by Hypoxia-Inducible Factor (HIF) Hydroxylases: Unique or Ubiquitous? Cells. 2019;8(5).

147. van Staalduinen LM, Jia Z. Post-translational hydroxylation by 2OG/Fe(II)-dependent oxygenases as a novel regulatory mechanism in bacteria. Front Microbiol. 2014;5:798.

148. Hirsila M, Koivunen P, Gunzler V, Kivirikko KI, Myllyharju J. Characterization of the human prolyl 4-hydroxylases that modify the hypoxia-inducible factor. J Biol Chem. 2003;278(33):30772-80.

149. Jaakkola P, Mole DR, Tian YM, Wilson MI, Gielbert J, Gaskell SJ, et al. Targeting of HIF-alpha to the von Hippel-Lindau ubiquitylation complex by O2-regulated prolyl hydroxylation. Science. 2001;292(5516):468-72.

150. Voit RA, Sankaran VG. Stabilizing HIF to ameliorate anemia. Cell. 2020;180(1):6.

151. Martin F, Linden T, Katschinski DM, Oehme F, Flamme I, Mukhopadhyay CK, et al. Copper-dependent activation of hypoxia-inducible factor (HIF)-1: implications for ceruloplasmin regulation. Blood. 2005;105(12):4613-9.

152. Yeo EJ, Cho YS, Kim MS, Park JW. Contribution of HIF-1alpha or HIF-2alpha to erythropoietin expression: in vivo evidence based on chromatin immunoprecipitation. Ann Hematol. 2008;87(1):11-7.

153. Wood SM, Gleadle JM, Pugh CW, Hankinson O, Ratcliffe PJ. The role of the aryl hydrocarbon receptor nuclear translocator (ARNT) in hypoxic induction of gene expression. Studies in ARNT-deficient cells. J Biol Chem. 1996;271(25):15117-23.

154. European Association for Study of L. EASL Clinical Practice Guidelines: Wilson's disease. J Hepatol. 2012;56(3):671-85.

155. Chen N, Hao C, Liu BC, Lin H, Wang C, Xing C, et al. Roxadustat treatment for anemia in patients undergoing long-term dialysis. N Engl J Med. 2019;381(11):1011-22.

156. Gomes A, Dedoussis GV. Geographic distribution of ATP7B mutations in Wilson disease. Ann Hum Biol. 2016;43(1):1-8.

VITA

Nikita Santosh Gudekar was born on October 21st ,1989, in Mumbai, India. She received her Bachelors in Biotechnology degree from the University of Mumbai. Nikita continued her studies to pursue a Masters degree (MS) in Biotechnology from Dr. D.Y. Patil of the Institute of Biotechnology and Bioinformatics. She graduated with a Masters degree in June 2013. Since 2015, she has been a Ph.D. student in the Genetics Area Program (GAP) at the University of Missouri-Columbia.